

AD-A238 223



1



DTIC
ELECTE
JUL 22 1991
S D D

THE SELF-SHIELDING OF FALLOUT
GAMMA RAYS BY TERRAIN ROUGHNESS

THESIS

Mark S. Herte
Captain, USAF

AFIT/GNE/ENP/91M-2

DISTRIBUTION STATEMENT A

Approved for public release
Distribution Unlimited

DEPARTMENT OF THE AIR FORCE

AIR UNIVERSITY

AIR FORCE INSTITUTE OF TECHNOLOGY

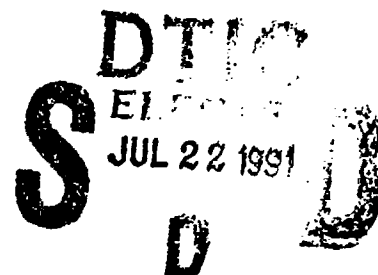
Wright-Patterson Air Force Base, Ohio

91-05727



91 7 19 127

AFIT/CNE/ENP/91M-2



THE SELF-SHIELDING OF FALLOUT
GAMMA RAYS BY TERRAIN ROUGHNESS

THESIS

Mark S. Herte
Captain, USAF

AFIT/CNE/ENP/91M-2

Approved for public release; distribution unlimited

91-05727


91 7 19 127

AFIT/GNE/ENP/91M-2

**The Self-shielding of Fallout Gamma Rays
by Terrain Roughness**

THESIS

Presented to the Faculty of the School of Engineering
of the Air Force Institute of Technology
Air University

In Partial Fulfillment of the
Requirements for the Degree of
Master of Science in Nuclear Engineering

Mark S. Herte, B.S.N.E.
Captain, USAF

28 FEBRUARY 1991

Accession For	
NTIS	DTIC
DTIC	DTIC
DTIC	DTIC
Justification	
By	
Distribution	
Availability Codes	
Dist	Avail and/or Special
A-1	

Approved for public release; distribution unlimited



Preface

The purpose of this study was to provide a first order calculation of the self-shielding of fission fragment gamma rays due to small surface irregularities, or "roughness". To simulate actual fallout, polymer microspheres were deposited on samples of soil, concrete, and asphalt roofing shingles. A scanning electron microscope was then used to photographically map the surfaces. Next, the photographs were "digitized" to allow measurement of microscopic surface irregularities as "seen" by the microspheres. Finally, the self-shielding due to surface roughness was calculated for each of the surfaces using the Monte Carlo transport code, MORSE.

Many people contributed to the successful completion of this study, and I would like to thank a few of them. First, I thank Karen Teal of Wright Research and Development Center's Materials Characterization Facility, who provided both the equipment and training necessary to characterize the samples. Thanks also to Capt Mike Howard, Lt Cmdr Kirk Mathews, and Maj Denis Beller for their help with MORSE. Special thanks to Dr. Charles Bridgman for his guidance and encouragement. Finally, to my wife Samantha, thank you for enduring these months of "wife neglect".

Table of Contents

Preface	ii
Abstract	vi
I Introduction	1
Background:	1
Purpose and Scope:	3
II Theory	6
Dose Rate:	6
Monte Carlo:	10
Self-shielding:	15
III Methods of Analysis	18
Homogeneous Buried Source:	18
Surface Mapping:	24
Measuring Roughness:	30
Surface Modelling:	33
Self-shielding Calculations:	35
IV Results and Discussion	37
Homogeneous Buried Source Results:	37
Surface Characterization Results:	40
Surface modelling Results:	56
Self-shielding Results:	61
V Conclusions and Recommendations	64
APPENDIX A: Roughness Data	68
APPENDIX B: MORSE User Written Subroutines	74
APPENDIX C: Sample MORSE Input	88
APPENDIX D: Gamma Source Emission Rates	93
APPENDIX E: Davies McDonald Fall Mechanics Code	95
Bibliography	98
Vita	101

Table of Figures

Geometry for MORSE Calculations	19
Albedo Boundary Simulating Infinite Plane Source	21
Mean Particle Radii Grounding in 24 Hours	26
SEM Setup	29
Measuring Surface Roughness With Cue 2	32
Normalized Dose Rate	39
SEM Photo of 22 Micron Particles on Soil	43
SEM Photo of 40 Micron Particles on Soil	44
SEM Photo of 77 Micron Particles on Soil	45
SEM Photo of 165 Micron Particles on Soil	46
SEM Photo of 22 Micron Particles on Concrete	47
SEM Photo of 40 Micron Particles on Concrete	48
SEM Photo of 77 Micron Particles on Concrete	49
SEM Photo of 165 Micron Particles on Concrete	50
SEM Photo of 22 Micron Particles on Shingles	51
SEM Photo of 40 Micron Particles on Shingles	52
SEM Photo of 77 Micron Particles on Shingles	53
SEM Photo of 165 Micron Particles on Shingles	54
Plot Comparing Model Geometries for Soil	59
Plot Comparing Model Geometries for Shingles	60

Table of Tables

Composition of Soil and Air	22
Average Measures of Roughness	56

Abstract

The purpose of this study was to provide a first order calculation of the self-shielding of nuclear weapon fission fragment gamma rays by surface roughness (microscopic terrain irregularities). To simulate fallout particles, 22, 40, 77 and 165 μm (diameter) polymer microspheres were deposited on slides containing samples of soil, concrete and asphalt roofing shingles. A scanning electron microscope was then used to photographically map the surfaces. Next, the photographs were converted to binary files to allow computer image processing. The Olympus metallurgical software, Cue 2, was used to quantify the roughness of each surface by measuring the thickness of surface irregularities at various angles as "seen" by the particles. Measurements showed a dependence upon the surface type, but not upon particle size. Average values of the measurements were modelled by a plane geometry of uniform thickness. That is, surface roughness was modelled as an infinite plane, 58 microns thick for soil and 211 microns thick for the shingles (roughness of the concrete samples was negligible). With this geometry, dose rates were calculated using the Monte Carlo transport code, MORSE. The MORSE calculations showed self-shielding due to roughness of not more than five per-

cent for the soil samples and eight percent for the shingles. The 30 percent self-shielding used in The Effects of Nuclear Weapons for level terrain is six times as great. It is postulated the large attenuation formerly attributed to roughness may actually be an artifact of an incorrect global/local fallout partition.

I Introduction

Background:

The value of fallout models may be measured by their ability to accurately predict radiation doses to targets at various locations. But even complex models, often referred to as "full physics codes", contain many assumptions and engineering estimates. The degree of self-shielding by the ground, the partition between local and global fallout, the exclusion of fission products inconsequential to the source spectrum and the simplification of radiation transport mechanisms are all examples of such assumptions. If predictions disagree with values measured in the field, correction factors are introduced to adjust the calculations. Ground self-shielding (terrain roughness factor) is the assumption critically examined in this thesis.

Because fallout models typically assume the particles land on a perfectly smooth surface, a correction factor for terrain roughness seems a sensible choice. Here, terrain roughness refers to irregularities in the surfaces upon which fallout particles are grounded. Obviously, mountains, canyons and buildings will greatly perturb dose rates in their vicinity, but many have argued that even small irregularities can cause significant attenuation. It is believed

self-shielding by agglomerations of soil particles, stones and organic matter cannot be neglected. In the widely used reference, The Effects of Nuclear Weapons, (ENW) by Glasstone and Dolan, a roughness factor of 0.7 is given for mildly rough terrain, and factors as great as 0.5 or 0.6 for rough terrain (9:453,428). Unfortunately, the authors fail to define mildly rough and rough, though the correction of 0.7 is also said to be appropriate for flat countryside (9:435). Further, the authors fail to show how these factors were calculated, leading one to suspect they are "engineering adjustments".

If terrain roughness can reduce dose rates by 50 percent, a more accurate means of estimating roughness factors should be of value. This study will accomplish a first pass at this task. Instead of using a fallout code to model the fallout gamma source distribution, it will be modelled as an infinite plane source with gamma emission rates (GER) and gamma energy spectra as determined by Millage (12). This source will be used with the Multigroup Oak Ridge Stochastic Experiment code (MORSE) running modified versions of the subroutines developed by Howard (6,10). The geometry module of these subroutines models the terrain as a perfectly smooth infinite plane of homogeneous soil upon which the

source rests. This module will be modified to model a rough surface. A geometry to model terrain roughness will be developed by characterizing samples of surfaces typically encountered in the Dayton Ohio area, namely soil, concrete and asphalt shingles (large scale perturbations caused by hills, buildings and trees will not be considered). Characterization of the surfaces will be accomplished using scanning electron microscopy (SEM) and computer image processing. The results of the characterization will be used to model the geometry of the surface's irregularities. This model will be used to perform Monte Carlo calculations to produce a first order estimate of the self-shielding by these surfaces.

Purpose and Scope:

The following steps were established for this study:

- (1) use the MORSE Monte Carlo transport code with a "buried source" model to perform an initial estimate of the attenuation of a gamma source transported through homogeneous soil as a function of soil thickness,
- (2) quantify the roughness of several surfaces upon which fallout particles might be deposited,
- (3) calculate the self-shielding due to the measured

roughness by equating it to a uniformly buried source,

(4) compare the results with those found in the literature.

As with any study of this nature, some approximations were necessary to make the problem tractable. First, the gamma ray spectra of the source determined by Millage did not include induced activity from the weapon itself (12). Since induced activity depends upon weapon design, this simplification may introduce errors in both the gamma emission rate and the spectra (Glasstone suggests neutron activation may add about 4% to the dose) (9:454). Second, the fission product calculations for U-235 and Pu-239 were based on thermal fissions, while those of U-238 were based on fast fissions. This was done because the codes used to calculate the fission products (DKPOWR and ORIGIN2) do not contain the cross section or fission yield data for weapon energy neutrons. However, according to T. England of the Los Alamos National Laboratory, the fission products and their decay characteristics are both more dependent upon the type of fuel than upon the neutron energy (12:3).

Since the total cross sections of materials in the transport media vary considerably over the energy range of interest, even slightly inaccurate source spectra could

introduce significant errors (6:137-139). Of greater concern however, is the use of a source homogeneously distributed over an infinite ground plane without hills, vegetation or other "large scale" perturbations to the topography. Allowing for variation in the source distribution would produce "hot spots" in areas of greater concentration (possibly the result of rain out), while the presence of large attenuators would produce areas of much lower dose rates (shadowing). Both these limitations must be kept in mind, but to address them further is beyond the scope of this study.

Another assumption implicit in this study is that surfaces where the particles might ground are typified by those randomly selected from the Dayton, Ohio area. In fact, fallout clouds may transport debris for thousands of miles in the 24 hour period over which "local" fallout may be deposited (3:9). Because of the diversity of terrain over such a large expanse, this study could not address all the possible permutations. Because of this, care must be taken in applying the results of this study to surfaces different than those examined. Additional assumptions will be stated where applicable.

II Theory

Dose Rate:

Dose rate is a measure of the rate of energy deposition by radiation per unit mass of a given target. Understanding the possible effect of terrain roughness on fallout gamma dose rates, requires first understanding how these dose rates are normally calculated.

As with all radiation dose calculations, a fallout dose calculation begins by specifying a radiation source. Any such source can be described by its type, distribution (energy, spatial and angular) and intensity. Fallout source distributions are a function of weapon yield, atmospheric and meteorological conditions, and terrain, while emission rates and energy spectra are functions of the weapon design, height of burst and time elapsed since burst (9). In general, dose rate calculations are performed using approximations to the actual distribution and source intensity. For example, it is common practice to model the distribution as an isotropically emitting infinite homogeneous plane with an activity as expected one hour after detonation (unit-time reference activity, UTRA) (9:390). For simple gamma dose calculations a UTRA of 530 gamma-megacuries per kiloton fission yield with an average photon energy of 0.7 MeV is used

(the gamma-megacurie is a unit introduced in ENW and corresponds to an emission rate of 3.7×10^{16} gammas per second) (9:453). Since attenuation cross sections are dependent upon photon energy, and many different energies are present in the decay chain, the use of a single average photon energy may be inaccurate. Greater accuracy may be achieved by using unclassified approximate gamma emission rates and spectra, such as calculated by Millage (12). However, as noted previously, even these source parameters do not match any actual weapon source (12:3).

The standard target is a tissue equivalent point suspended one meter above the source plane. Given such a target, a specified fallout source, and the composition of the medium (media) through which the radiation passes to reach the target, the dose rate can be calculated. The calculation involves transporting the radiation quanta from the source to the target and calculating the response of the target to the radiation reaching it. Clearly, not all the radiation emitted by the source will reach the target. Geometric considerations alone preclude this. In addition to geometric attenuation, the radiation must usually pass through a medium (media) with which it will interact. In the case of photons (gamma radiation), the quanta may either

reach the target without interacting, scatter toward or away from the target, or be absorbed by the medium before reaching the target. The equation solved in calculating dose rate is given as Equation 1.

$$\dot{D} = \int_0^\infty R(E)\phi(E) \quad (1)$$

Where

\dot{D} = Dose Rate to the target

$R(E)$ = Energy dependent target response

$\phi(E)$ = Energy dependent photon flux at the target

If the energy dependence can be discretized, equation 1 can be written as

$$\dot{D} = \sum_{i=1}^N R_i \phi_i \Delta E_i \quad (2)$$

Equation 2 divides the energy spectrum into N groups, each with a width ΔE . With this multigroup approach, the energy dependent response functions are typically evaluated at the center of each group using tabulated data for a given target material. The energies used are those of the photons at the target, not at the source. Calculating the flux, the number and energy of the photons reaching the target per unit time, requires a transport calculation. The discretized form of the transport equation is given as Equation 3.

$$\phi_i = \sum_{j=1}^N t_{ij} q_j \Delta E_j \quad (3)$$

Where

t_{ij} = Transport function, the probability of transporting radiation energy (per unit photon energy) from the source in energy group j to the target in energy group i

q_j = Source photon energy in energy group j

ΔE_j = Bin width of energy group j .

Evaluation of the transport function can be accomplished using one of several different techniques. In the simplest transport approximations the scattered contribution to the dose rate is neglected and the average energy of the spectrum is used, rather than the multigroup structure. That is, a total average removal cross section is used in the transport function and no allowance is made for scattered photons reaching the target. This calculation is accomplished using Equation 4.

$$t_{ij} \approx \int_{s_1}^{s_2} \frac{e^{-\mu_{t,avg} s'}}{4\pi s'^2} 2\pi s' ds' \quad (4)$$

where

s' = Slant range through the particular medium

s_1 = Point where the photon enters the medium

s_2 = Point where the photon leaves the medium

μ_{avg} = Total removal cross section for the medium at the average energy of the spectrum.

The failure to account for scattered photons reaching the target results in a dose rate that is less than the true dose rate. More refined techniques attempt to include the scattered contribution. Three of the most common means of accomplishing this are the use of a multiplicative build-up factor, or BUF, the method of successive scatters, and Monte Carlo computer codes. A discussion of the BUF and successive scatter methods can be found in Howard's thesis (10). In this study, the Monte Carlo method was used to perform all transport calculations.

Monte Carlo:

The Monte Carlo technique is the most realistic transport technique available. The term Monte Carlo is derived from the technique's use of random numbers to determine the outcome of stochastic processes. The method consists of actually following each of a large number of particles from "birth" at a user-specified radiation source, throughout its life history, to its "death" in one of a number of possible ways. This process is accomplished with high-speed digital computers programmed to simulate the actual physical pro-

cesses that govern the particle's behavior. That is, for a particular type of radiation transport, say gamma, a life history of each photon is recorded as it travels from collision site to collision site. To accomplish this, the course, or "random walk", of each particle's life is simulated with elementary probabilities of interaction for a given particle, in a particular medium, with a specified geometry. The term "random walk" refers to the zigzag path a photon travels during its life because of scattering events.

Typical Monte Carlo computer codes divide the entire process into a number of subroutines. The process begins with the generation of a particle by the Source subroutine. Because a particle is characterized by its position and direction coordinates as well as its energy, these parameters are assigned to each particle at birth by the Source subroutine. Random number generators are used to decide which values, from a preset list for each parameter, will be assigned to a given particle. The particle is created with an initial energy and trajectory, and its information is passed to the Random Walk subroutine.

The Random Walk routine decides whether a particle reaches the boundary to the next zone without incident, or

experiences a collision while traversing the zone. This too is a stochastic decision, based upon the particle's mean free path within the particular medium. The program proceeds with a calculation of the particle's parameters at the site of the collision or boundary crossing (5:12).

In the case of a collision, the values are passed to the Collision subroutine. This routine determines the nature of the collision and thus the particle's immediate fate. A particle's life may be terminated as the result of a collision, or if it leaves the system. "Death" as a result of collision occurs if the particle's weight is too low to continue tracking it (discussed later). In either case, the appropriate category for the termination is incremented and the program loops to create another particle. If the particle survives, it continues with a new trajectory and energy. With these new parameters, the random walk continues.

As mentioned previously, the use of random numbers is essential to the Monte Carlo method. For example, they are used to determine the path length and trajectory traveled by particles traversing a particular medium. The path length is described by the function in equation 5, and is based upon the mean free path of the particular type and energy

radiation in the particular medium. Equation 6, gives the probability, P , of the particle traveling some distance, s , without interacting with the medium (10:11).

$$s = -\ln(r)/\mu \quad (5)$$

$$P = e^{(-\mu s)} \quad (6)$$

where

P = Probability of no interaction in a path length s

s = Path length

μ = Total cross section

r = A random number on the interval $0 < r < 1$.

To calculate the trajectory, the program generates random numbers, n , such that $-1 \leq n \leq 1$. These numbers are used as direction cosines, which in conjunction with the path length, are used to determine the next collision/boundary crossing.

Because the Monte Carlo calculation is stochastic, the answer it gives is not unique. Rather, it is an estimate that lies within a statistical confidence interval around the true answer. Obviously, the greater the number of particle histories followed, the more precise the result. However, following more particles takes more computer time. Because of this, other more efficient methods of variance

reduction are often used to achieve better results in less time. There are several variance-reduction techniques commonly used, among them are Russian roulette and splitting.

When a collision occurs, the particle's weight is reduced. In terms of computational efficiency, following low-weight particles from site to site until they are finally either absorbed or escape the system is very inefficient. Russian roulette is a technique used to avoid tracking low-weight particles. Each time a particle survives a collision, its new weight is checked against a user-assigned value. If the new weight is less than this value, Russian roulette is initiated. The procedure uses an operator-assigned-chance-of-survival, x , (where $0 < x < 1$) and a computer-generated-random-number (also between 0 and 1). If the random number is greater than the survival value, x , the particle is "killed". As with all particle "deaths", the appropriate termination category (in this case Russian roulette kills) is incremented. If on the other hand, the random number is less than the survival value, the particle survives with an increased weight. The weight increase is also a user-assigned value (5).

Splitting is another common variance reduction technique. This technique is used to improve the accuracy of

results by increasing the number of particles in certain user-specified "key" regions, without introducing unwanted particles everywhere in the system. Typically, the key regions contain some target or detector, the response of which is desired. The procedure requires the operator to divide the system into various importance regions. When a particle enters a new region, its weight is checked against an operator-assigned value for that region. If the particle's weight is greater than this value, the particle is split into two separate particles, each having half the weight of the original. The process is repeated until the weights of all new particles are less than the assigned value for the region. By creating twice as many particles, each with half the weight of the original, the total particle weight is unchanged, while the statistical variation for the region is reduced (16:294).

Self-shielding:

Terrain roughness can reduce the dose rate received by a target, by introducing an additional medium for the radiation to pass through (soil, concrete, etc.). In terms of the Monte Carlo technique, this is equivalent to adding another zone. While addition of this zone may not increase the linear distance to the target, it can cause a large

decrease in the radiation's probability of reaching it.

There are two factors responsible for this reduction.

Referring to equation 5, the path length of the radiation is a function of the total cross section μ . The total cross section is in turn a function of the particular medium as well as the energy of the radiation, as given by Equation 7.

$$\mu_m(E) = \sigma_m(E) \rho_m \quad (7)$$

Where

$\mu_m(E)$ = The macroscopic total attenuation cross section of medium m at energy E

$\sigma_m(E)$ = The microscopic total attenuation cross section of medium m at energy E

ρ_m = The atomic density of medium m.

The effect of density on path length is obvious. As the density of the medium increases, the atoms become more closely packed, thus increasing the likelihood of a collision. Because the density of any surface irregularity will greatly exceed that of air, the additional zone will have a larger macroscopic cross section, which will cause significant attenuation over even a short distance.

It is often more convenient to express the total attenuation cross section, μ , as a density specific cross section (mass attenuation coefficient). This is accomplished by

dividing μ by the density of the medium. Since Compton scattering depends only upon the number of electrons present, and Z/A is about $1/2$ for all materials except hydrogen (over the range where the Compton process is dominant) the mass absorption coefficients will be approximately constant (14:120).

This approximation is made more convenient by the introduction of another term, the mass integral, MI . The mass integral of a particular medium is given by Equation 9.

$$MI_m = \int \rho_m ds \quad (9)$$

Where

MI_m = Mass integral of medium m

ρ_m = Density of medium m

ds = Incremental path length

Because Compton scattering is the dominant interaction mechanism over the gamma energy range of interest, the mass attenuation coefficients are roughly constant. Thus, an approximation of the self-shielding provided by a particular medium is reduced to a dependence upon only the density and thickness of the medium. These values are conveniently represented by the mass integral of the medium.

III Methods of Analysis

Homogeneous Buried Source:

A series of Monte Carlo calculations were performed to estimate the size of the terrain irregularities required to produce the amount of self-shielding cited in ENW. This initial estimate was required to bound the problem. That is, it provided a simple method of determining what sort of surface would significantly attenuate fallout gammas. A uniformly buried source model was used with the MORSE Monte Carlo code to calculate the attenuation by homogeneous soil of three different gamma sources calculated by Millage (8:6,12). A standard soil composition was obtained from the Radiation Shielding Information Center (RSIC) at Oak Ridge National Laboratory. The geometry shown in Figure 1 depicts the buried source model used. The model consists of an infinite homogeneous plane gamma source buried beneath varying depths of homogeneous soil. The source is surrounded above by a thin layer of soil and then an infinite volume of air, and beneath by an infinite volume of soil. A detector is located one meter above the ground. Composition of the soil and air are given in Table 1 (10:20). If the depth of burial is taken as zero, then the calculation repeats Howard's calculations.

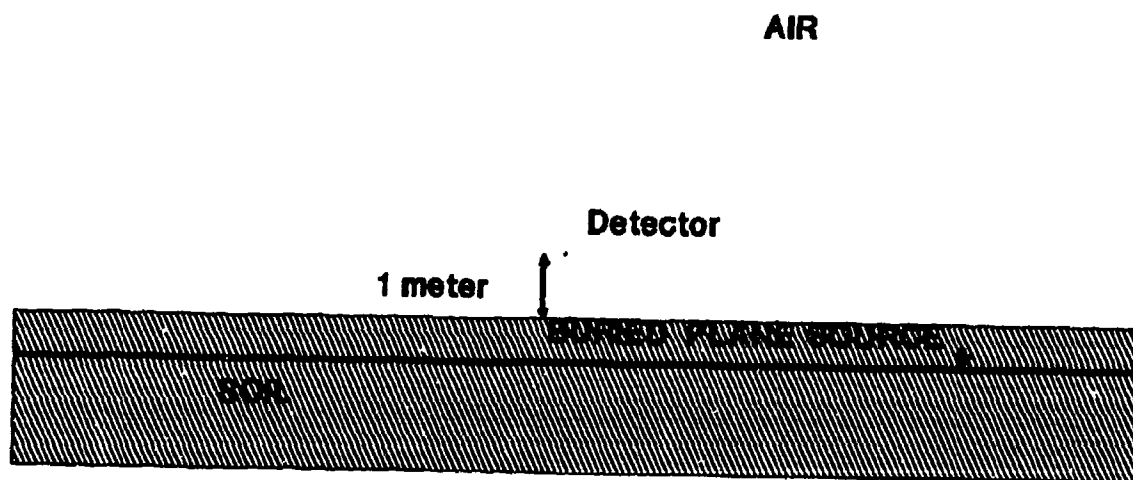


Figure 1
Geometry for MORSE Calculations

With these input parameters, the Monte Carlo transport code MORSE was used to calculate the decrease in the dose rate at the detector as the thickness of the soil covering the source was increased (the source was more deeply buried).

The package of MORSE subroutines written by Howard were modified to accomplish this initial estimate of self-shielding. These subroutines are reproduced in Appendix C. The package includes a combination of subroutines and input data required to model an infinite homogeneously distributed plane source placed at various depths beneath the surface. The infinite plane source is modelled with a point source centered on a one square kilometer plane with a perfect albedo surface on all sides. The albedo feature permits the isotropic point source to mimic an infinite plane source. As seen in Figure 2, the mirror-like reflection of the photons when striking the albedo surface simulates the emission of photons from an infinite homogeneous plane source (7). Use of a boundary crossing flux estimator (in the BDRYX subroutine), located one meter above the ground plane, permits estimation of the flux by dividing a weighted number of particles that cross the boundary by the area of the boundary.

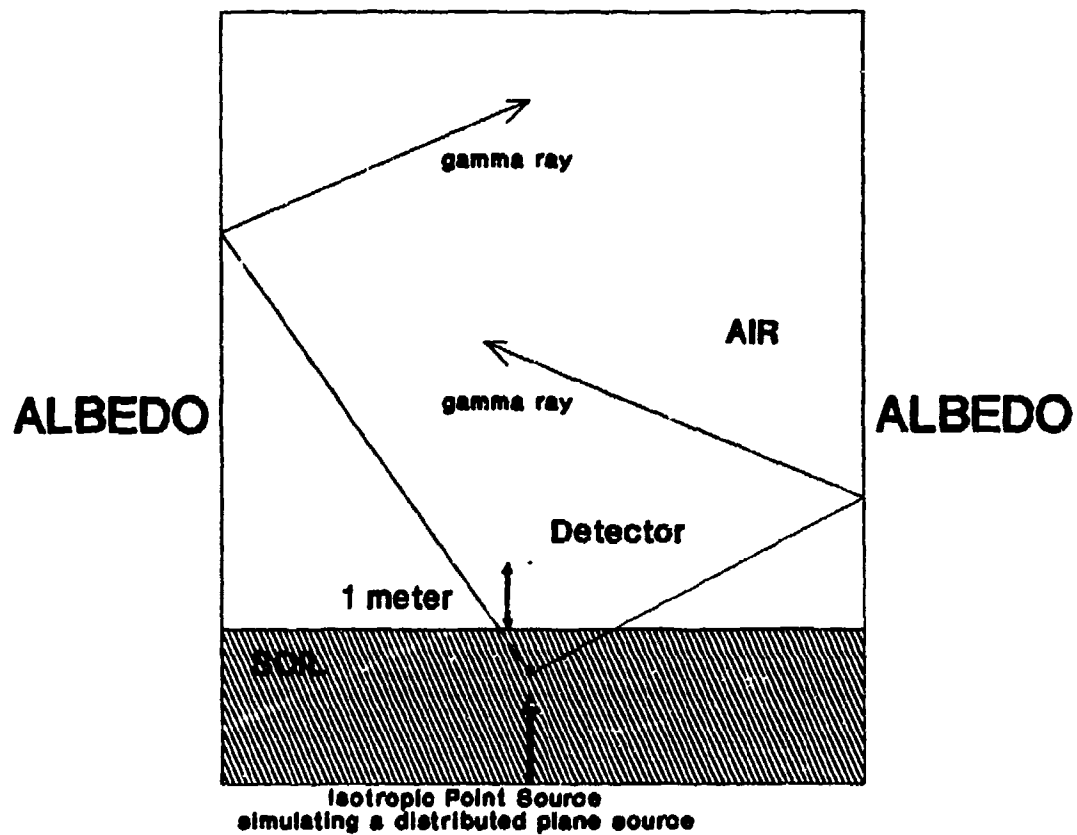


Figure 2
Albedo Boundary Simulating an Infinite Plane Source

Weighting is accomplished at each crossing of the boundary using a factor of $|1/\cos\alpha|$ where α is the direction of motion measured away from the vertical.

Table 1

Composition of Soil and Air Used in MORSE Calculations

Element	Air		Soil	
	Atomic Density (Atoms/cm ³)	Fractional Composition	Atomic Density (Atoms/cm ³)	Fractional Composition
H			9.752E+21	.160
N	4.199E+19	.784		
O	1.128E+19	.211	3.480E+22	.570
Al			4.880E+21	.080
Si			1.160E+22	.190
Ar	2.515E+17	.005		

The U-235, U-238 and Pu-239 spectra and GER's calculated by Millage were changed by Howard from a nineteen gamma energy group structure to a twenty-one group structure (10).

This restructuring allows use of the FEWG1 cross section library with the MORSE code (2). The FEWG1-85 cross section library is a cross section library developed for the Defense Nuclear Agency and is available through RSIC. It contains 37 neutron energy groups and 21 gamma energy groups, though only the gamma energy groups were used in this study.

To convert the energy structures to twenty-one groups, Howard assumed each of the nineteen energy bins had an equal gamma emission rate for all energies within the individual group. That is, if the energy bin had to be divided into two equal energy bins in the new structure, half of the gammas would be placed in one bin and half in the other. In addition, because the FEWG1 structure does not support photon energies below three keV, it was assumed no fission products emitted a gamma with an energy lower than three keV. Again, as noted by Howard, this can be verified by examining the chart of the nuclides (13). The spectra used in this study are included in Appendix D.

Both the cross sections and the response functions use the twenty-one energy group structure. The response functions used were the Henderson gamma free-in-air tissue kerma values (2:76-79). These values have units of $\text{rads-tissue}/(\text{gamma-cm}/\text{cm}^3)$ indicating they are normalized

per source photon. To calculate the actual dose rate from the MORSE output, the target response must be multiplied by the fluence at the target. However, because this study was concerned only with the change in the dose rate with increasing surface roughness, actual dose rates were never calculated. Rather, all results were normalized by dividing the target response for the rough surface calculation by the response for the perfectly smooth surface.

Surface Mapping:

The results of the homogeneous buried source calculations provided an estimate of the thickness of surface irregularities necessary to cause the self-shielding reported in ENW. The next objective was to compare this roughness estimate with actual surface roughness. This second phase began by quantifying the roughness of some random samples of surfaces found in the Dayton, Ohio area. To accomplish this, samples of soil, concrete and asphalt roofing shingles were collected. Though none of these samples had large surface irregularities, they were chosen as typical of the surfaces fallout would encounter in the Midwest.

To help characterize fallout deposition on the samples, four vials of non-radioactive fluorescent polymer micro-

spheres were purchased from Duke Scientific Corporation, Palo Alto, CA. Each vial contained one gram of microspheres (approximately 10^6 - 10^8 microspheres per gram) in sizes of 22, 40, 77 and 165 microns diameter. A range of particle sizes was purchased, because the size of "local fallout", ie. fallout grounding in the first twenty four hours after detonation, will vary greatly with time, as shown in Figure 3. This figure was calculated using the fall mechanics developed by Davies and McDonald (3:14). A listing of the Basic program used to generate Figure 3 is reproduced in appendix E. Though actual fallout particles are generally not spherical, sprinkling microspheres on the samples was deemed suitable for a first order estimate of true fallout distributions.

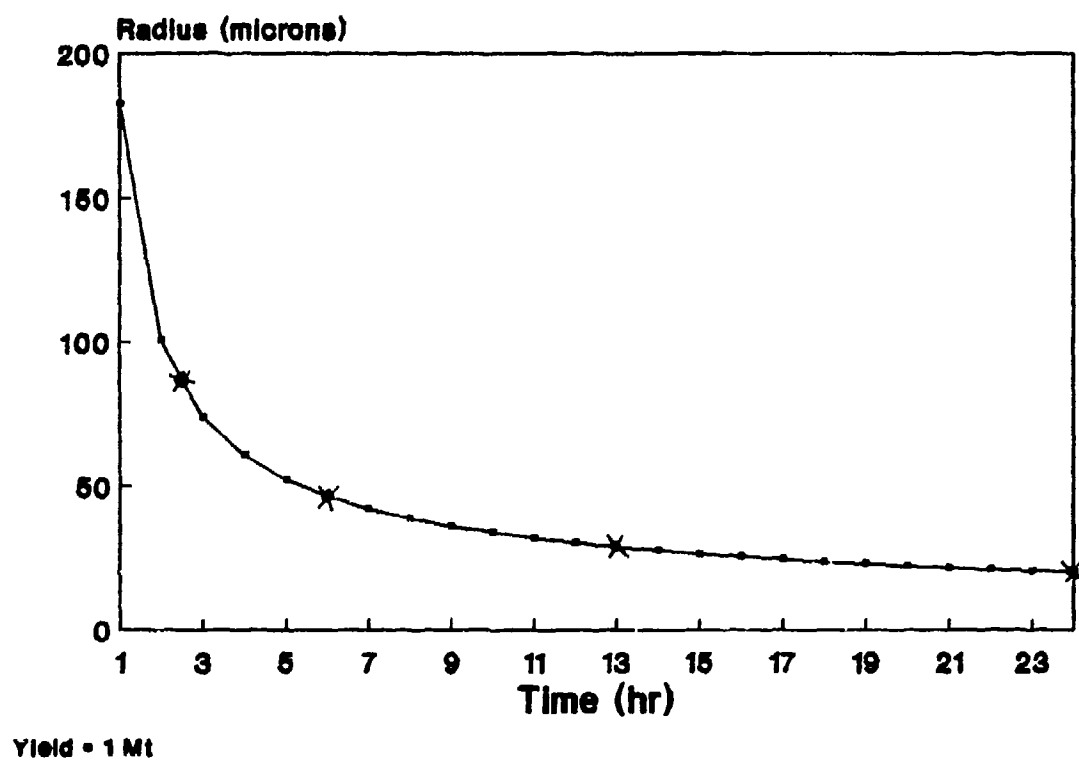


Figure 3
Mean Radii of Particles Grounding within
24 Hours of Detonation
as a Function of Time Since Detonation

While collecting the surface samples and microspheres was painless, deciding on a method for quantifying the roughness of the surfaces was a challenge. After considering the alternatives, microscopic photographing of the samples was chosen as the best means of accomplishing the task. However, resolving the details of the photography was also a challenge. The amount of magnification, the best viewing angle and even the type of microscope to use were all decided by trial and error. Because the samples had to be viewed in many different positions, they were fixed (using epoxy) to pieces of molybdenum the size of standard microscope slides. This provided a rigid sample that could be manipulated for viewing at any angle, while not altering the texture of the surfaces. Four samples of each surface were prepared in this way, one sample of each surface for each size microsphere. The microspheres were deposited on the surfaces by dropping them from a height of one meter and allowing them to free fall to the surfaces. Because of their small size, terminal velocity was achieved quickly and impact effects were negligible.

Though magnification of Fifty X seemed sufficient to photograph even the smallest microspheres, numerous attempts using optical microscopy proved inadequate due to depth of

field limitations. Switching to an ETEC Autoscan scanning electron microscope (SEM), provided both higher resolution and greater depth of field, but required additional sample preparation. Before the samples were placed in the SEM, a six-angstrom coating of gold was sputter deposited upon them using a Hummer sputtering system. The gold coating was used to reduce irregular charging of the surfaces by the electrons, thus providing clearer photographs.

While photographs of the surfaces as viewed directly from above were interesting, they did not permit measurement of surface irregularities. However, by placing the samples on edge, the topography was better discerned and measurement of the irregularities as "seen" by the microspheres appeared possible. Changes in the particles positions on the rotated surfaces were negligible, because of the coating and what appeared to be a static attraction to the surfaces. As shown in Figure 4, once the surfaces were ready, they were "mapped" by taking several SEM photographs of each.

Evacuated Chamber

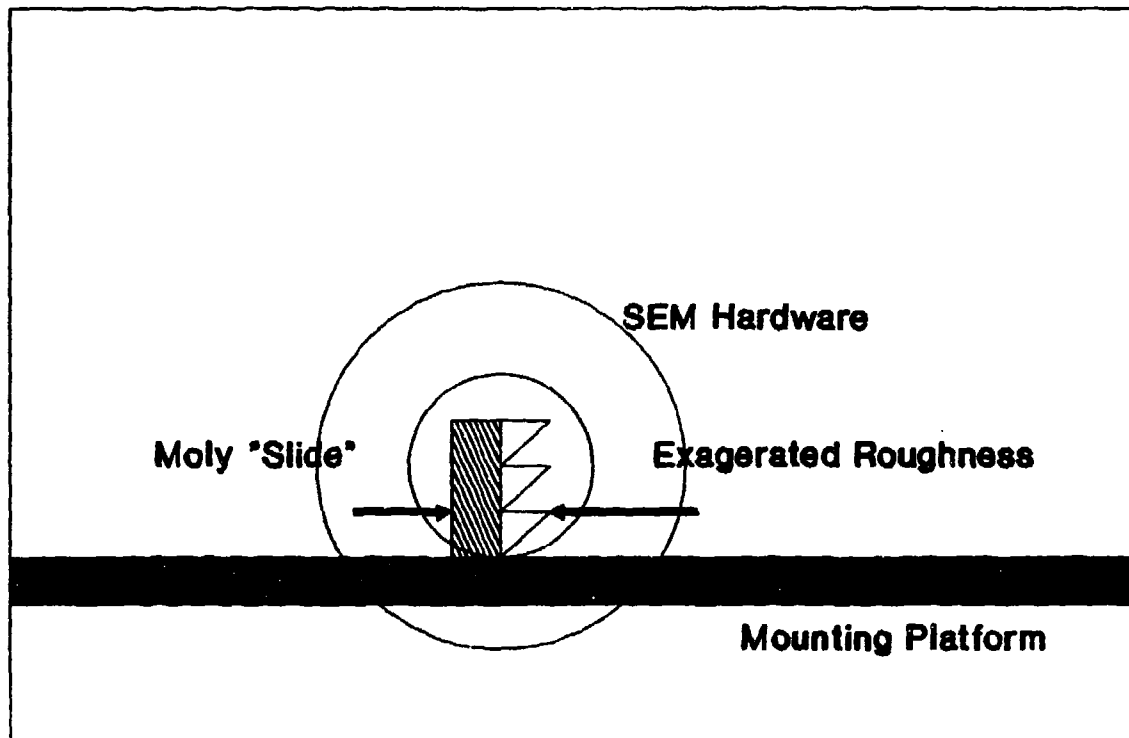


Figure 4
SEM Photographic Mapping Setup

Measuring Roughness:

After the surface mapping was finished, a means of measuring the surface irregularities revealed by the photographs was required. The Olympus metallurgical software package, Cue 2, was used to do this. The software was resident on an MSDOS based PC which was coupled to a video camera. The camera was used to convert the photographs into video signals which were fed to the PC for conversion to binary files by the software. Once in binary form, the photographs were enhanced, increasing the contrast and sharpening the edges of the surface irregularities.

The roughness measurements began by using a mouse to move the cursor around the digital image. A microsphere (in the image) was selected at random, and the cursor was anchored to the center of it. The software then created a display at the bottom of the screen which showed the cursors position in units of microns from the anchor point and degrees from horizontal. Again using the mouse while watching the display, the cursor was moved out from the particles center at a fixed angle, θ , as shown in Figure 5. If at any point on this trajectory the cursor passed through some surface material, the thickness of the material was noted by recording the change in the cursors position while passing

through the material. The cursor was moved in this fashion until it was completely clear of the surface. That is, the surface roughness was measured at specific angles by measuring the thickness of surface irregularities as viewed by the microspheres. This procedure was repeated for angles of 22.5, 45, 67.5, 90, 112.5, 135 and 157.5 degrees from the horizontal. Once the measurements were complete for a given particle, another particle was selected and the process repeated. The procedure continued until twenty particles were measured from each of the twelve different surface/microsphere combinations.

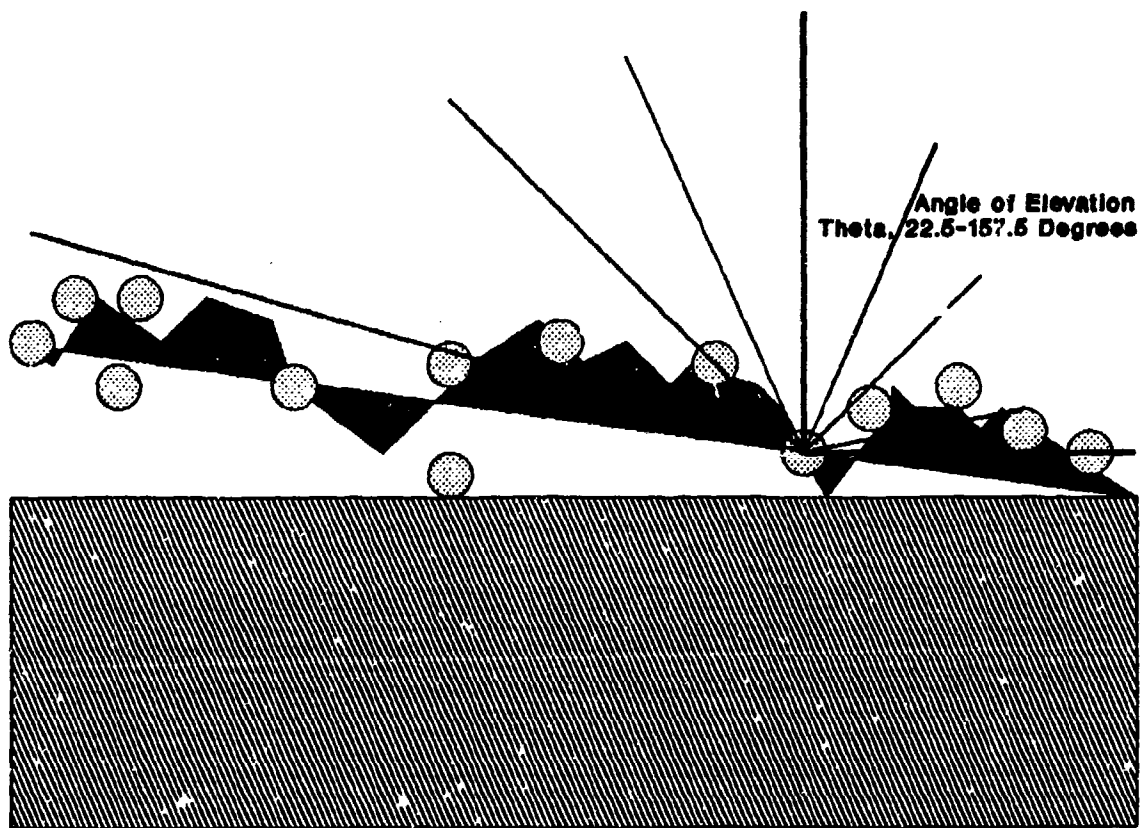


Figure 5
Measuring Surface Roughness Using Cue 2 Software

Surface Modelling:

After completing the measurements, average values and standard deviations for each group of measurements were calculated using the built in statistics functions on a Hewlett Packard HP-15C. That is, all the measurements at a given angle for a given surface were averaged. Then, to increase the number of data points at each angle and to take advantage of symmetry, the measurements from the supplementary angles of each surface (opposing angles that sum to 180 degrees, Eg. 22.5 and 157.5) were also averaged.

A rigorous model of the averages of the measured values for a given surface would require a fine mesh (large number of different angles) and the use of a weighting scheme to properly represent the average thickness at each angle. Use of such a complex model however, would not be justified in light of the inherently large variation in the measurements. This large variation is due to the presence of particles on top of the surface. Such particles will not be shielded, thus they will produce a zero thickness measurement at all angles. Other particles will be shielded at some angles, but not at others. Therefore, a rigorous model of the rough surface geometries would be over-kill.

To provide a simple, yet accurate model, two different versions of the homogeneous buried source model used previously were used to model each of the heterogeneous surfaces. This was done by equating the average values of the measured thickness (at each angle) of each surface's irregularities to homogeneous burial-depths. Although a single homogeneous Right Parallelepiped (RPP) could not duplicate the average measurements of any of the surfaces at all angles, by constructing two different RPP models for each surface, one thicker at some angles than the average measurements, and one thinner, the true self-shielding by each surface was bounded.

The RPP models used were infinite planes of each surface material with thickness' determined as follows:

(1) For the "thin" RPP's, the average values of each surface's thickness measurements at 90 degrees were used as the thickness of the corresponding RPP. Use of RPP's with these uniform thickness' accurately modeled the average surface thickness measurements near 90 degrees, but underestimated them at smaller angles.

(2) For the "thick" RPP's, the average values of each surface's thickness measurements at 22.5 degrees were used to calculate the thickness of the corresponding RPP. The

thickness was calculated assuming the 22.5 degree values were the length of the hypotenuse of a right triangle with a 22.5 degree angle of elevation. The uniform thickness of the corresponding RPP was then equal to $x \sin(22.5)$, where x was the average thickness of the 22.5 degree measurement. Use of RPP's of this uniform thickness accurately modeled the average surface thickness measurements near 22.5 degrees, but overestimated them at larger angles.

Self-shielding Calculations:

Self-shielding by each of the surfaces was calculated using the MORSE transport code with each pair (thick and thin) of the homogeneous RPP geometries and the appropriate cross sections. Although the cross sections for soil had been mixed when the first series of self-shielding calculations (using the buried source) were performed, cross sections for concrete and shingles had yet to be prepared. Preparation of cross sections for any material requires knowledge of the atomic densities of the material. While the data for concrete was available in the MORSE manual, no reference for the composition of the asphalt shingles could be found. After talking with a chemist from the Georgia Pacific Corporation, a large manufacturer of shingles, it was apparent the roughness of the asphalt shingles was due

entirely to the presence of the calcium carbonate aggregate (15). Based upon this information, the thin coating of asphalt covering the aggregate was neglected and the shingles were modelled as pure calcium carbonate. The cross sections were mixed using the XCHKR routine with data as shown in appendix B.

IV Results and Discussion

Homogeneous Buried Source Results:

A series of Monte Carlo calculations were performed to estimate the size of the terrain irregularities required to significantly attenuate fallout gammas. A buried source model was used with the MORSE Monte Carlo code to calculate the attenuation by homogeneous soil of three different gamma sources. The results of this initial estimate of surface roughness are presented in Figure 6. The graph shows the attenuation of U-235, U-238 and Pu-239 gamma sources by simulated terrain roughness. Increasing degrees of surface irregularity were simulated by altering the MORSE geometry module to bury the gamma sources beneath various depths of an infinite plane of soil. The calculated dose rates have a statistical error less than one percent. Once calculations were completed, the results were normalized by dividing the dose rate for each calculation by the dose rate for a source on a perfectly smooth surface. The normalized values are graphed as a function of the surface roughness. As expected the dose rate to the target decreases with increasing thickness of soil (greater surface roughness). At large values of thickness, the values for the U-238 source differ from those of the U-235 and Pu-239 sources by about nine percent.

The difference is due to the harder spectrum of the U-238, hence greater ability to penetrate. Thickness in Figure 6 is given in units of mass integral thickness, g/cm^2 . For all sources, the figure clearly shows significant attenuation for sufficiently rough surfaces. The half thickness, the value at which the gamma source is reduced by one-half, occurs at $1.7 \text{ g}/\text{cm}^2$ soil for all three sources. This value corresponds to 1 cm of reference soil with a bulk density of $1.71 \text{ g}/\text{cm}^3$. The reduction to the value used in ENW for "typical flat countryside", 0.7 of the ideally smooth surface, requires a mass integral thickness of $0.5 \text{ g}/\text{cm}^2$, or 0.3 cm (3,000 microns) of soil.

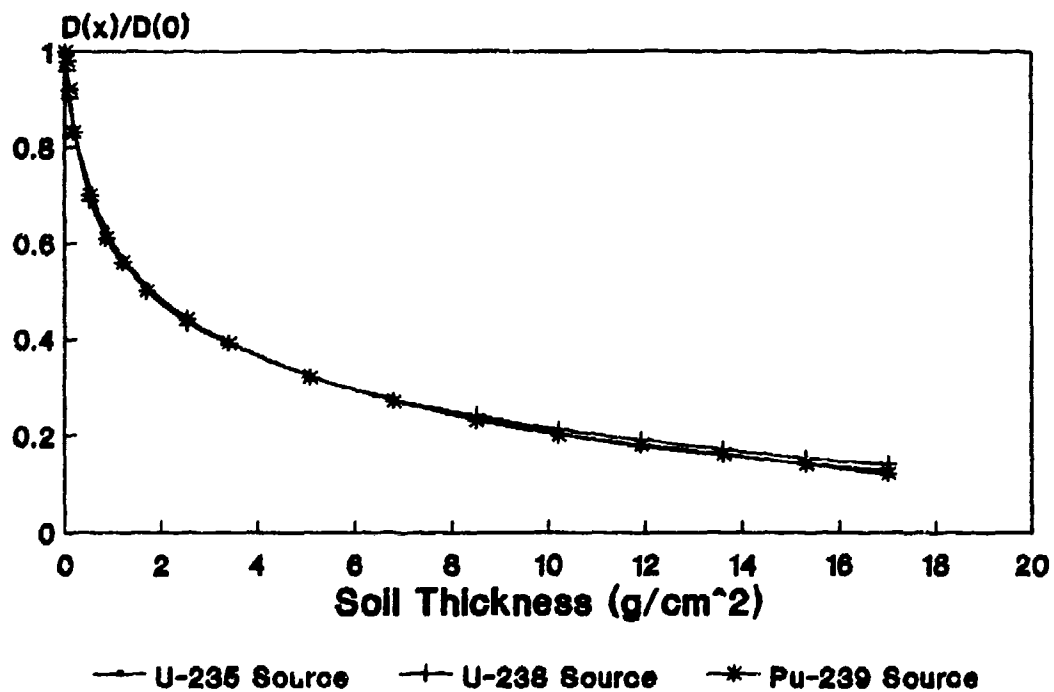


Figure 6
Normalized Dose Rate as a Function of Simulated
Surface Roughness Using Variably Thick Planes of Soil

Surface Characterization Results:

The initial calculations quantified the magnitude of the surface roughness required to produce sizable self-shielding. Next, a study of some sample surfaces was performed to determine whether a typical surface would have a wealth of 3,000 micron deep crevices large enough to accommodate local fallout sized particles. This next phase also determined whether modelling surface roughness as a right parallelepiped, regardless of the thickness used, was unrealistic.

SEM microscopy and digital image analysis were used to characterize the roughness of some typical surfaces. In the process of characterizing the surfaces, some additional observations were made. For example, When the microspheres were deposited on the surfaces, they tended to collect near pointed projections. This was especially true of the smaller particles. One possible explanation for this is the presence of a static charge on the microspheres. Static attraction would be less pronounced in larger particles, because their weight would overcome the small electrostatic force. This phenomenon would likely have an even greater effect upon actual fallout particles, where the longer free-fall could generate greater surface charging. Coupled with

the presence of grass and other vegetation, this could significantly perturb the particle distribution and lower the expected self-shielding.

Another possible perturbation to the simulated fallout distribution may have occurred when the samples were placed in the SEM. Because the samples were placed on edge, some change in particle positions may have occurred. Even if the force of gravity alone was not enough to perturb the microspheres, once the samples were placed in the SEM the chamber containing them was evacuated. Both these problems were mitigated by the use of the gold coating, though the initial change in air pressure did dislodge some of the larger particles. This is evidenced by the surreal "satellites" seen floating above the landscape in some of the photos. While this dislocation does alter the particle distribution, the microspheres most likely to succumb to the vacuum are those on top of the surfaces. Again, loss of these particles causes an overestimate of the self-shielding of the surface.

Twelve of the photographs taken using the ETEC Autoscan SEM are reproduced in Figures 7 - 18. Each photograph is of a different surface/microsphere size combination. The photographs were all taken viewing the samples on edge, as if looking from the side at ground level. Magnifications

ranged from 20X to 50X. The figures show the particles distributed over the surfaces such that some are completely shielded from above, while others rest atop the surface, exhibiting no shielding at all. Some of the figures (eg. figure 7 and others) show particles below the horizon that stuck to the edge of the mounting slide; these particles should be ignored. Again, the presence of grass or other organic matter covering most soil would normally catch much of the fallout and thus reduce the shielding effect of the surface because of the relatively low densities of these materials. Obviously the asphalt exhibits the greatest amount of surface roughness, while the concrete appears smooth. Another collection of samples may have produced different photographs. Clearly the limited number of samples analyzed suggests the results must be taken as merely first-order.

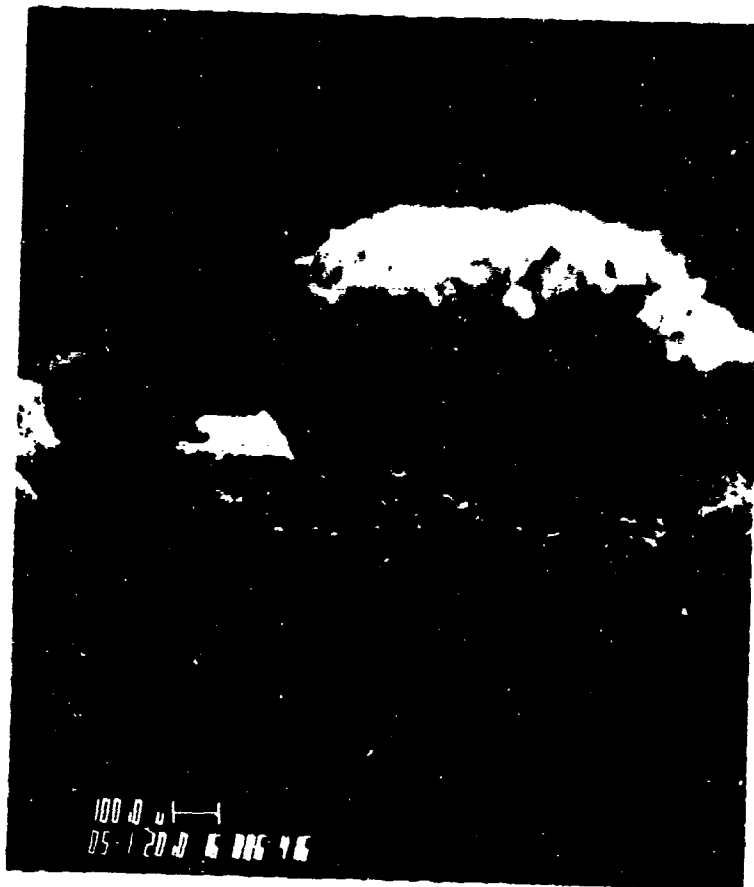


Figure 7
SEM Photo of 22 Micron
Particles on Soil

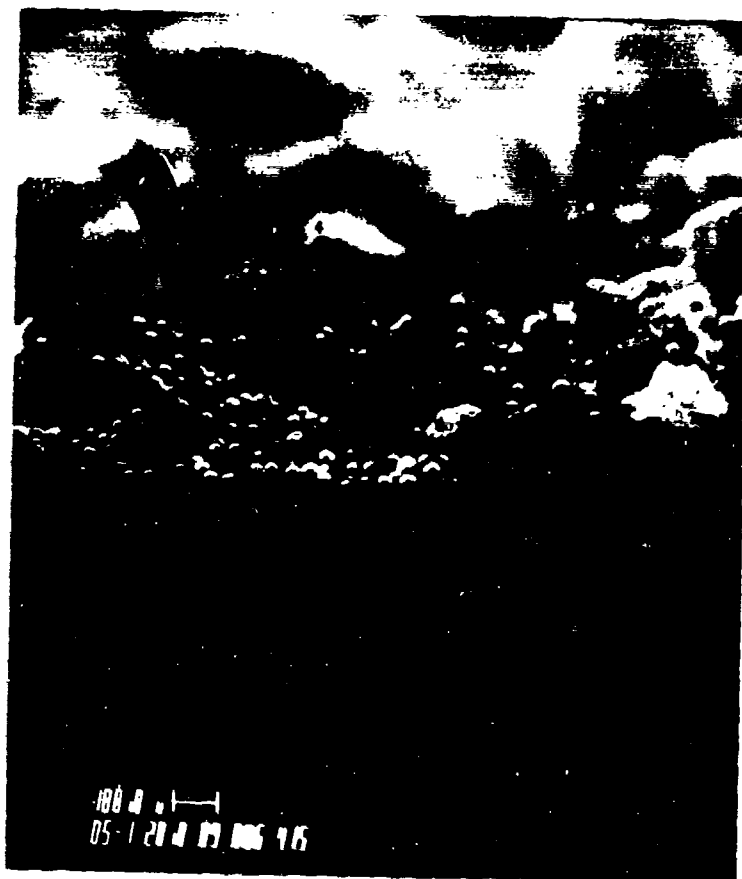


Figure 8
SEM Photo of 40 Micron
Particles on Soil



Figure 9
SEM Photo of 77 Micron
Particles on Soil

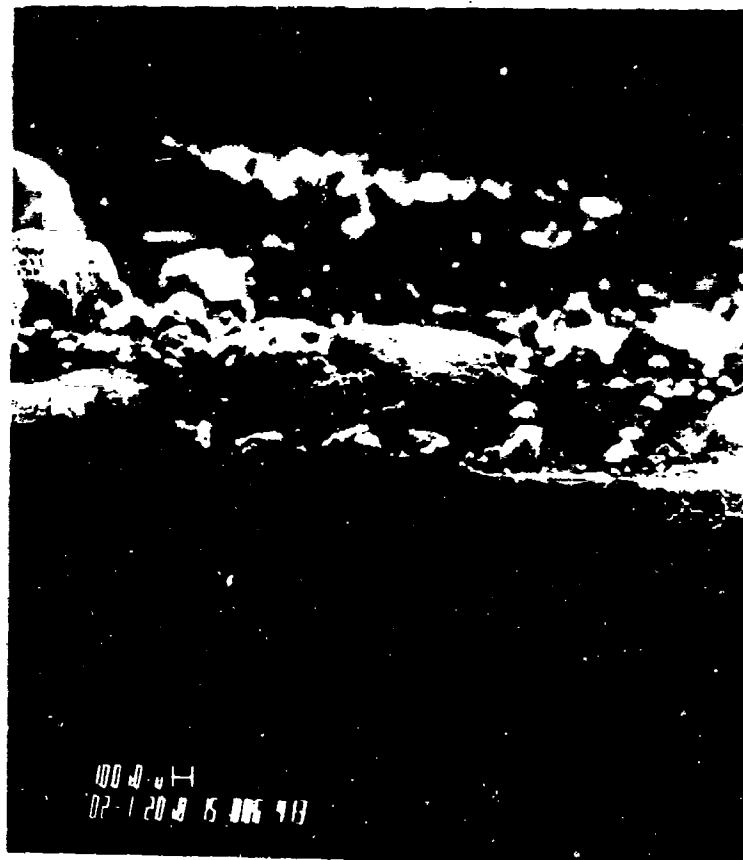


Figure 10
SEM Photo of 165 Micron
Particles on Soil

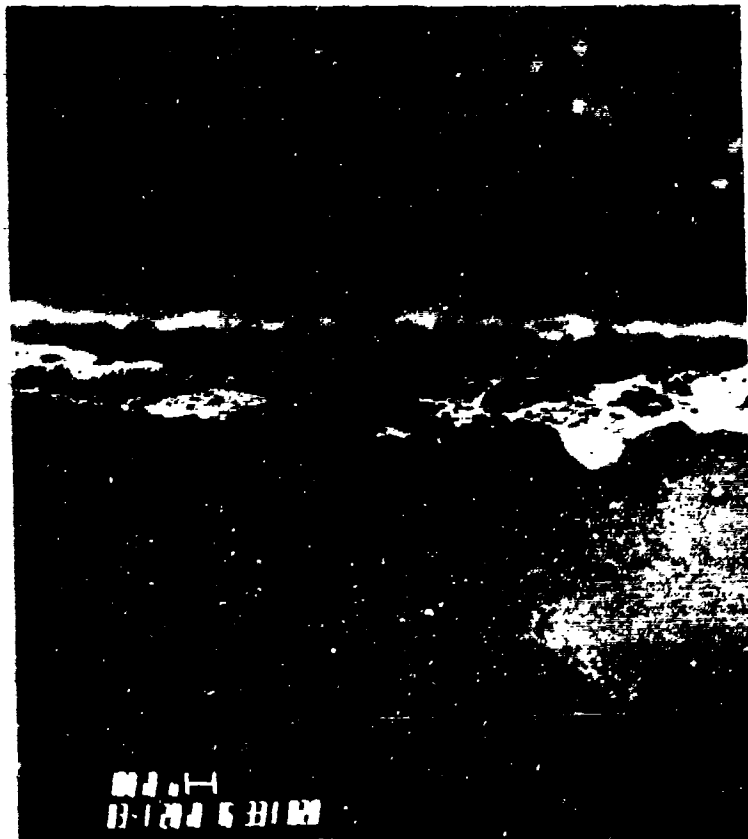


Figure 11
SEM Photo of 22 Micron
Particles on Concrete

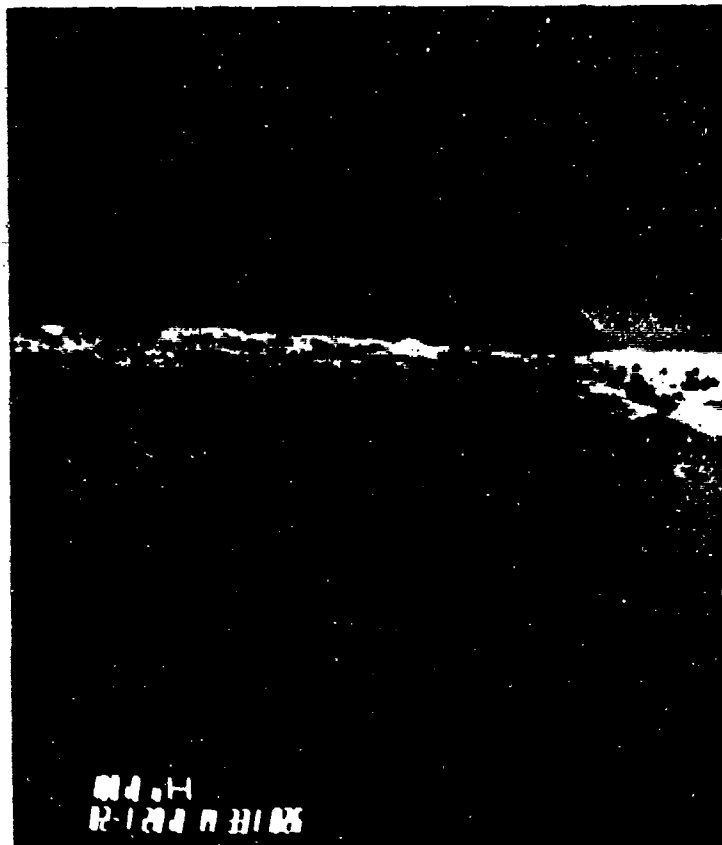


Figure 12
SEM Photo of 40 Micron
Particles on Concrete



Figure 13
SEM Photo of 77 Micron
Particles on Concrete

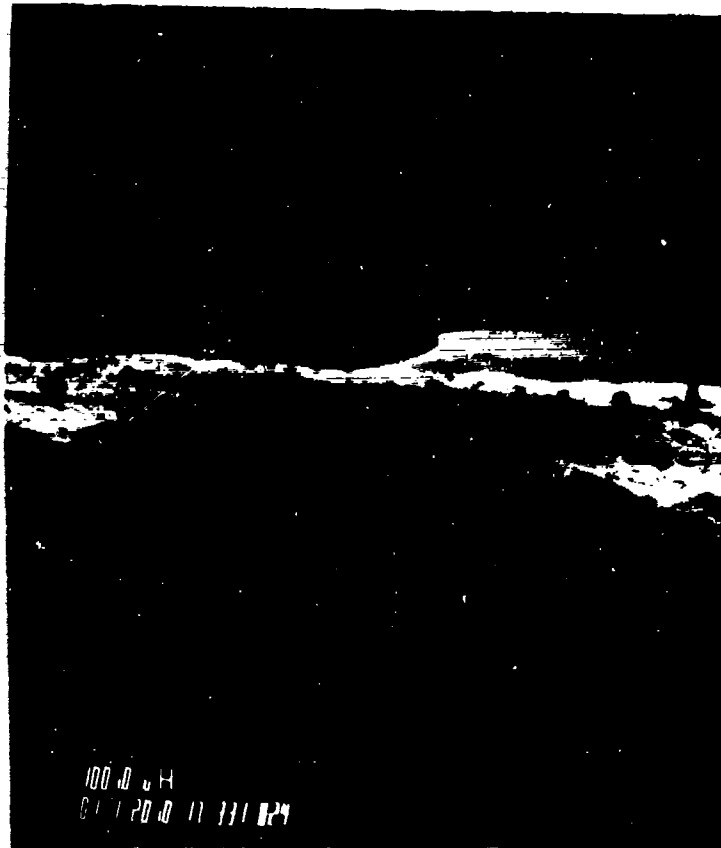


Figure 14
SEM Photo of 165 Micron
Particles on Concrete

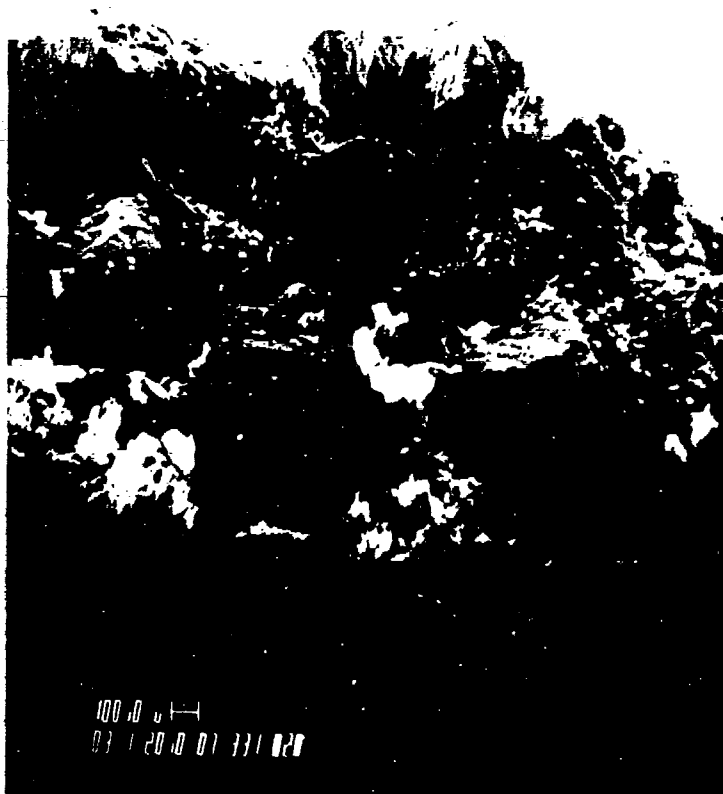


Figure 15
SEM Photo of 22 Micron
Particles on Shingles

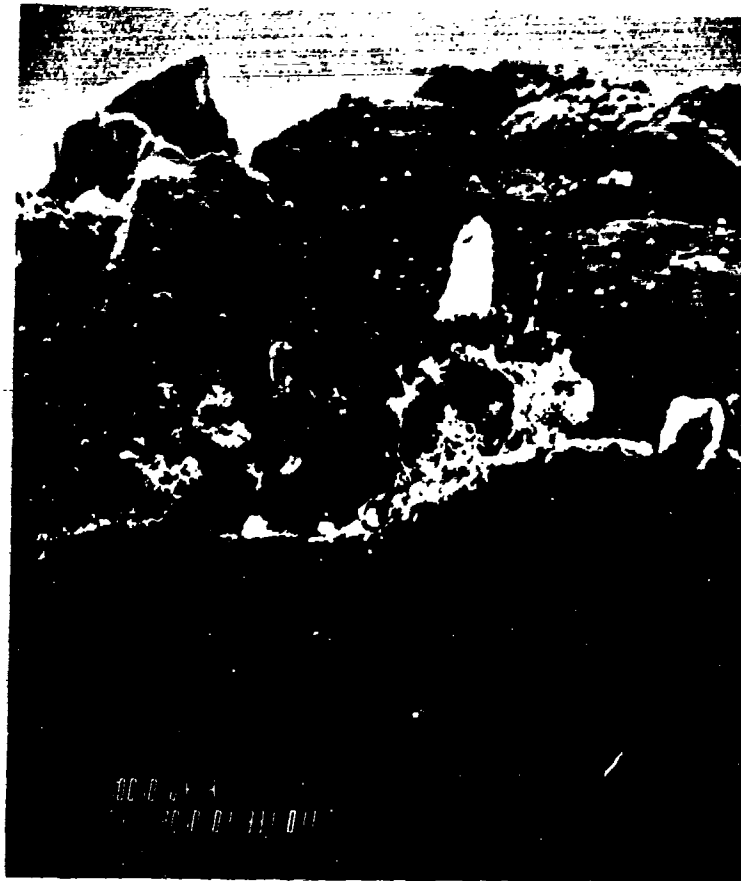


Figure 16
SEM Photo of 40 Micron
Particles on Shingles

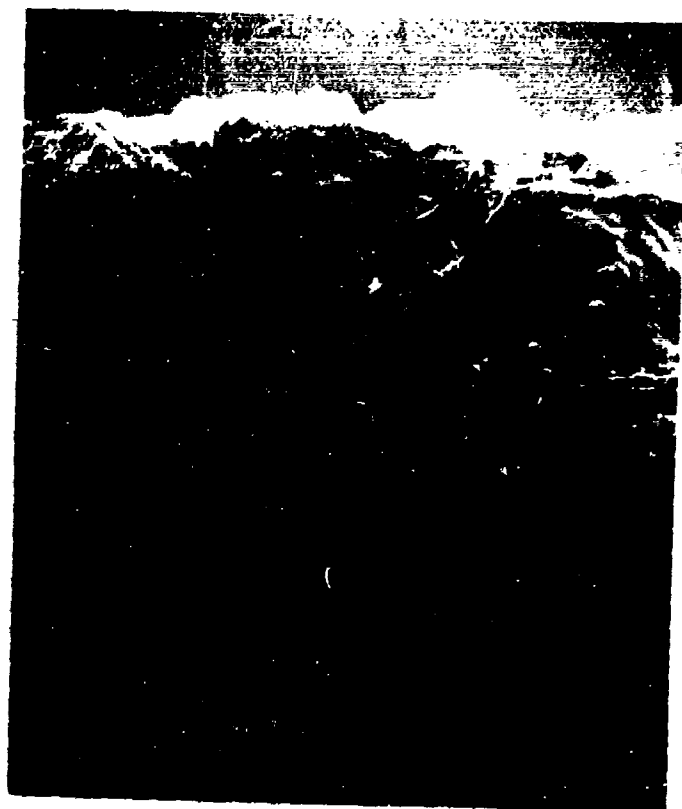


Figure 17
SEM Photo of 77 Micron
Particles on Shingles

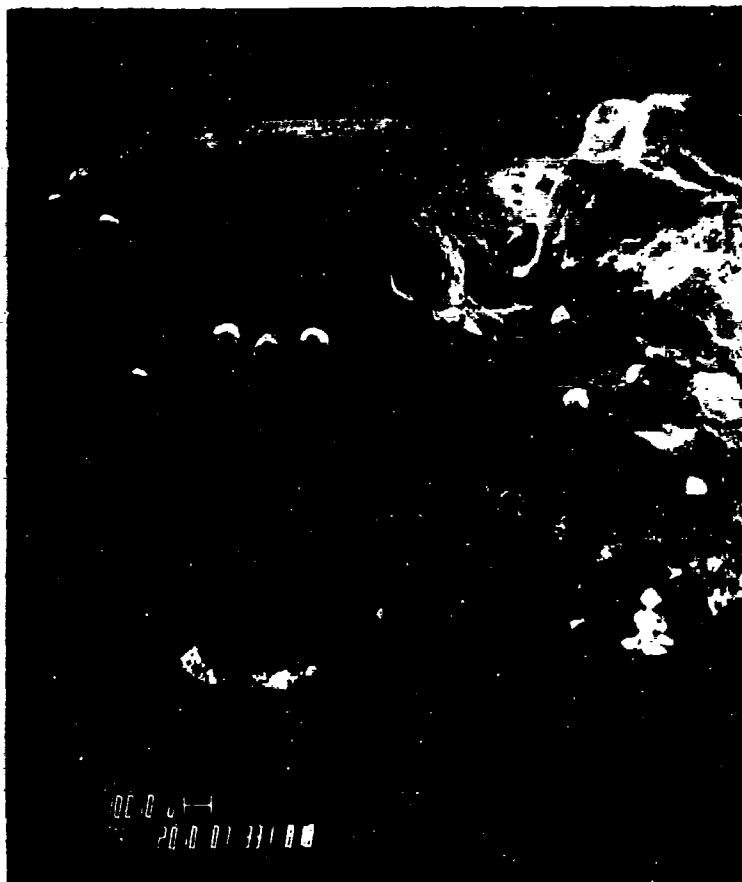


Figure 18
SEM Photo of 165 Micron
Particles on Shingles

Measurement of the surface irregularities began by noting a few prominent features. The deepest crevices noted in the asphalt samples were approximately 350 microns beneath the surrounding surface. The maximum shielding such a surface could provide would occur if all debris was deposited in these crevices. That is, a calculation based on this assumption will yield the upper bound for a surface roughness factor for asphalt shingles. The soil samples were generally very smooth, but had occasional large agglomerations of soil particles which would cause some attenuation. Results of the measurements for soil and the shingles are included in appendix A. The roughness of the concrete samples was negligible. Average values and standard deviations of the measurements appear in Table 2.

Table 2
Average Measures of Surface Roughness for Asphalt Shingles
and Soil

Theta (Degrees)	Average Thickness (microns)			
	Soil		Shingles	
	<i>X</i>	<i>Sx</i>	<i>X</i>	<i>Sx</i>
22.5	264	262	533	532
45	117	204	364	372
67.5	78	170	270	282
90	58	155	211	241

Surface modelling Results:

The large standard deviations were a result of the great disparity in self-shielding experienced by individual particles. Some particles were completely shielded, while many others were not shielded. In light of the large standard deviations, use of the simple homogeneous buried source models discussed in chapter III was appropriate. Constructing a model geometry to accurately duplicate the inhomogeneous topography would require a greater number of angles and the use of a weighting scheme to assign surface thickness values

as a function of the view angle. Figures 19 and 20, compare the geometries used to bound the surface roughness factors for the soil samples and the shingle samples. The figures show the average values of the measurements for each surface plotted as a function of the view angle θ . Shown with these plots are the upper and lower bound homogeneous buried source values actually used in modelling the geometry for the Monte Carlo calculations.

The upper bound set of values produces an overestimate of the self-shielding, because it overestimates the thickness of the surfaces at large values of θ . That is, a homogeneous RPP with a thickness matching the measured values at 22.5 degrees, has a thickness greater than the measured values at 90 degrees. This greater thickness will produce more attenuation than would the actual surface. In contrast, the homogeneous RPP's used to calculate the lower bounds of self-shielding, duplicate the measured surface thickness' at 90 degrees, but are less than the measured values at 22.5 degrees. Thus the lower bound calculation will under-estimate the self-shielding. Between the two models, the lower bound is probably more accurate. This is because θ is a function of the distance from the target (a smaller value of θ corresponds to a greater distance

from the target) and the contribution to dose rate decreases with increasing distance from the target. In fact, at distances greater than fifty meters from the source (theta less than two degrees elevation) the gamma contribution is negligible even without surface roughness due to the mean free path of gammas in air. Thus, inaccuracies in the surface roughness model are most pronounced when the gamma source is near the target. Inaccuracies are less pronounced at larger angles (which correspond to source points further from the detector) where the contribution to the total dose rate is less important.

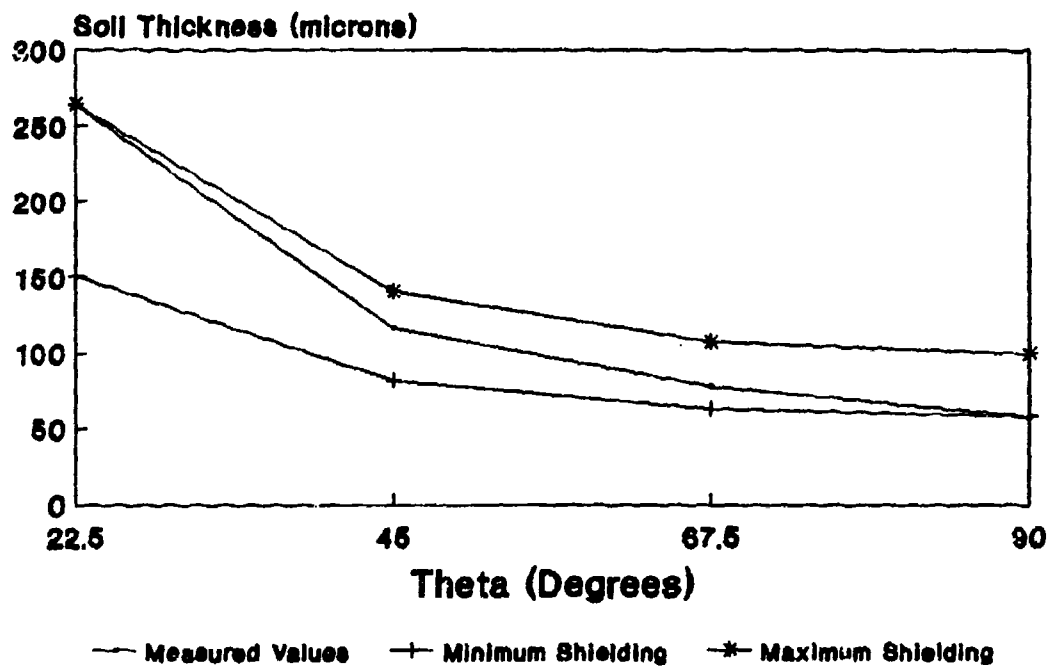


Figure 19
Plots of Model Geometries Used to Predict Upper and Lower
Bounds of Self-shielding by Soil Surface Roughness

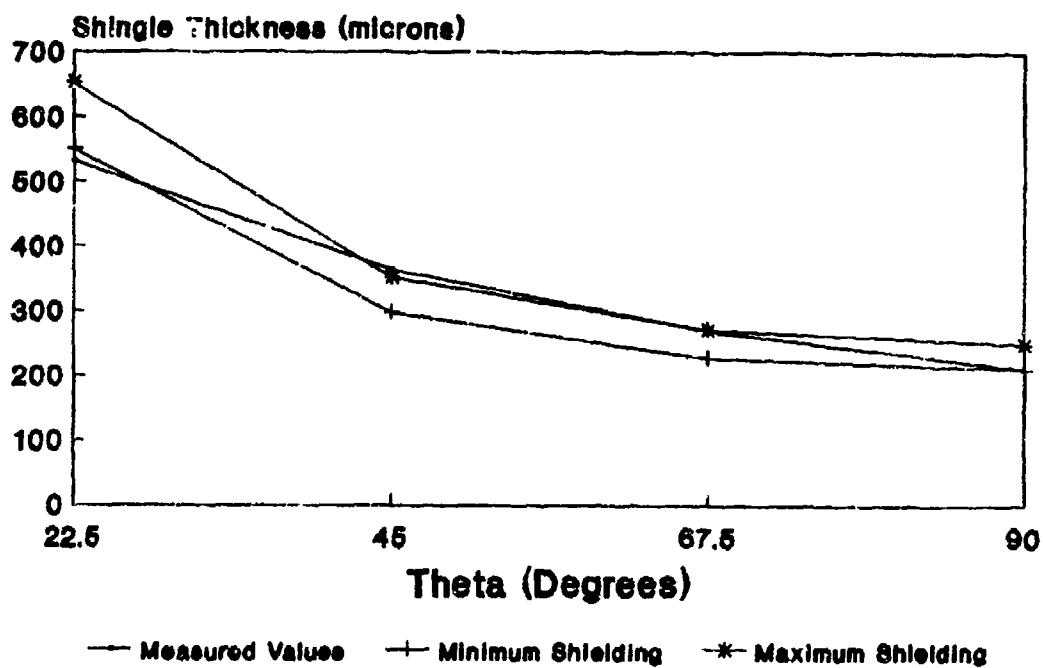


Figure 20
Plots of Model geometries Used to Predict Upper
and Lower Bounds of self-shielding
by Asphalt Shingles' Surface Roughness

Self-shielding Results:

The MORSE code was used to calculate the upper and lower bounds of self-shielding for the soil and shingle samples. Using the appropriate geometry and cross sections, the results were as follows:

1) For soil, the self-shielding was two to five percent, plus or minus the one percent statistical deviation of the calculation.

2) For the shingles, the self-shielding was five to eight percent, plus or minus one percent.

These values of self-shielding correspond to self-shielding factors (actually transmission fractions) of 0.98 to 0.92. By comparison, the self-shielding factor of 0.7 used in ENW for "typical flat countryside", suggests much greater attenuation than was found in this study.

Though there were many assumptions and approximations used in this study, most would cause an overestimate of the self-shielding. Even use of a model geometry with all particles located in the deepest crevices in the samples (200 - 300 microns) would fail to produce a self-shielding factor near the value used in ENW. As shown in Figure 6, a homogeneous RPP 3,000 microns thick would be required to produce this level of attenuation. One possible explanation for the

large disparity in the self-shielding values is the surfaces used in this study. All the surface samples used were relatively smooth. A rougher sample of concrete could have been used, or in addition to the common soil, a gravel covered surface could have been examined to model a rocky desert floor. Certainly a soil covered with small bits of rock averaging 1.0 cm or more in diameter could produce the level of attenuation suggested in ENW.

Another possible explanation for the large difference, is the idea mentioned in chapter one. Perhaps the self-shielding factor used in ENW was just a convenient choice of a multiplicative correction factor that forced the predicted dose rate calculations to match the measured values in the field. That is, the real cause of the disparity between measurement and prediction may be some assumption other than surface roughness, such as an incorrect global/local fallout partition. Studies have been carried out to better define global/local fallout, and all recognize the difficulties inherent in accurately predicting this partition (1). Because even small discrepancies in this value can cause large errors in calculations, an incorrect partition is also a possible explanation.

There are a number of other factors that could alter terrain self-shielding. Chief among these is weathering. Weathering could significantly alter the distribution of fallout on surfaces. Though not addressed in this study, weathering could dissolve some fallout carriers, washing the radioactive material into the soil, further increasing the self-shielding.

V Conclusions and Recommendations

The purposes of this study were as follows:

- (1) Calculate the attenuation of a gamma source transported through soil as a function of soil thickness.
- (2) Quantify the roughness of several surfaces upon which fallout particles might be deposited.
- (3) Assuming level terrain, calculate the self-shielding due to the measured roughness.
- (4) Compare the results with those found in the literature.

The MORSE Monte Carlo code, with modified versions of the subroutines written by Howard, was used to perform transport calculations from an infinite plane gamma source. The source, which used spectra and gamma emission rates calculated by Millage was buried beneath various depths of soil. This calculation provided a crude estimate of the mass integral thickness (roughness) of soil required to significantly attenuate the source. Results of these calculations showed a mass integral half thickness, the thickness required to reduce the source to one-half the unshielded value, of 1.71 g/cm^2 . The results also showed a mass integral thickness of 0.5 g/cm^2 would be needed to produce the roughness factor of 0.7 used by Glasstone and Dolan. This

mass integral thickness corresponds to a linear thickness of 3,000 microns of homogeneous reference soil. While this sort of surface is not common in the Midwest, a rocky desert or mountain soil could have an equivalent thickness this great, or even greater.

Having established the thickness required to produce sizable self-shielding, the next objective was to quantify the roughness of some random samples of surfaces found in the Dayton, Ohio area. For this purpose, samples of soil, concrete and asphalt roofing shingles were collected. Fall-out particles were simulated by depositing non-radioactive 22, 40, 77 and 165 micron (diameter) polymer microspheres on slides containing the sample surfaces. A scanning electron microscope was then used to photographically map the surfaces. Computer image processing was performed by converting the photographs to binary files. Image filtering and enhancement were accomplished using the Olympus metallurgical software, "Cue 2". Cue 2 was also used to quantify the roughness of each surface by measuring the thickness of surface irregularities at various angles as "seen" by the particles. The measurements showed no variation with respect to the particle sizes examined, but did vary considerably among the three surface types. The

asphalt was found to be the most rough, with an average linear thickness of 211 cm as measured directly above the fallout particles. The average thickness of the soil samples was 58 cm as measured directly above the particles, while the average value for the concrete was approximately zero.

Measuring the roughness of each surface allowed construction of a suitable geometric model. After evaluating the data averaged over each angle, it appeared the surface roughness of the soil and asphalt samples could be modelled as planes of uniform thickness. This lead to construction of MORSE input files modelling the roughness of the surfaces as infinite planes (right parallelepipeds), 58 microns thick for soil and 211 microns thick for the shingles (roughness of the concrete samples was negligible). A distributed homogeneous plane source was placed beneath the "rough" planes, and a plane of soil sufficiently thick to provide no leakage was placed beneath the source. With this geometry, The MORSE code was again used to calculate the reduction in dose rate.

The results of the MORSE calculations were not startling in light of the earlier buried source calculations performed. They showed surface roughness factors of not more

than 0.95 and 0.92 for soil and asphalt respectively. These values differ greatly from the 0.7 found in ENW. However, since Glasstone never clearly defines the terrain this factor is based upon, the large difference could be explained by assuming the value in ENW applies to a rocky terrain, atypical of the Midwest.

Certainly a more definitive explanation for the differences in the roughness factors should be explored. Though probably well beyond the scope of most facilities, another potentially beneficial study could benchmark the accuracy of these results by performing actual attenuation measurements using radioactive sources to simulate fallout. The material could be distributed over surfaces of variable roughness. A more realistic proposal for future study might be to address the effect of weathering on surface roughness. This issue was not explored in any detail; weathering could significantly change the value of the self-shielding factor.

APPENDIX A: Roughness Data

A.1 Soil Data

The following tables show the roughness of the different soil samples as a function of the angle, theta, measured in degrees.

Theta = 22.5 degrees							
Thickness (cm)							
192	347	254	276	636	492	96	369
0	0	0	0	384	200	744	391
213	254	318	186	0	1086	0	423
0	0	0	226	0	0	686	54
0	376	278	242	424	324	81	468
282	0	1100	232	368	142	233	0
981	210	188	306	0	338	167	639
969	246	340	0	0	0	460	0
278	249	544	0	186	354	114	474
341	137	564	0	258	412	0	0

Theta = 45 degrees							
Thickness (cm)							
360	220	198	246	0	0	0	453
254	0	0	0	0	0	96	0
0	580	216	0	0	0	0	0
0	0	0	0	0	0	0	0
228	0	0	0	0	245	0	0
0	0	642	0	85	0	0	504
0	0	0	208	898	283	354	0
0	0	284	0	882	348	60	0
0	0	528	0	237	182	405	0
0	0	0	0	251	123	0	0

Theta = 67.5 degrees							
Thickness (cm)							
280	0	210	202	0	0	0	319
180	0	0	0	0	0	0	273
0	0	0	0	0	0	0	0
0	0	0	0	0	0	0	0
0	0	0	0	0	0	0	0
0	0	268	0	0	0	0	0
0	0	0	192	740	590	293	0
0	0	246	0	732	603	30	0
0	0	444	0	0	90	363	0
0	0	0	0	112	46	0	0

Theta = 90 degrees							
Thickness (cm)							
0	0	112	222	0	0	0	263
108	0	0	0	0	662	0	0
0	0	0	206	0	667	0	0
0	0	0	0	0	0	0	0
0	0	0	0	0	76	0	0

A.2 Asphalt Shingles Roughness Data

The following tables show the roughness of the different asphalt shingle samples as a function of the angle, theta, measured in degrees.

Theta = 22.5 degrees							
Thickness (cm)							
431	680	952	928	600	660	707	1260
706	560	560	1018	628	0	1176	514
670	160	484	296	0	0	400	1442
825	0	838	0	646	0	1068	854
112	0	840	0	942	0	2347	1838
535	1092	0	0	614	0	1853	926
938	305	0	1096	1526	230	209	348
1067	367	0	330	348	0	1634	0
1132	0	0	120	0	0	874	0
965	0	470	208	0	0	300	0

Theta = 45 degrees							
Thickness (cm)							
317	676	380	0	674	672	823	360
383	359	554	0	502	0	703	350
235	0	292	0	0	0	923	718
150	0	854	0	416	0	880	588
0	0	220	0	798	0	1343	888
535	1092	0	0	456	0	538	694
938	305	276	678	774	92	0	312
1067	367	690	302	274	0	1202	0
1132	0	654	88	0	0	208	0
967	0	330	94	0	0	0	0

Theta = 67.5 degrees							
Thickness (cm)							
263	616	254	268	522	514	513	260
360	284	738	170	398	0	796	310
432	0	164	462	0	0	923	510
489	0	680	0	280	0	690	370
0	0	0	0	696	0	1021	608
209	660	0	0	276	0	570	592
465	223	0	148	894	0	0	316
509	97	0	0	276	0	0	0
595	0	0	412	0	0	0	272
647	0	540	0	0	0	0	268

Theta = 90 degrees							
Thickness (cm)							
230	638	0	0	0	136	661	302
443	235	552	0	604	0	642	378
473	0	184	0	0	0	450	460
559	0	326	0	0	0	0	0
0	0	460	0	416	0	0	294

APPENDIX B: MORSE User Written Subroutines

C.1 MORSE

C

C * * THIS IS THE MAIN ROUTINE * * * * *

C * * THE FOLLOWING CARD DETERMINES THE SIZE ALLOWED FOR
BLANK COMMON

C COMMON NC(200000)

C * * (REGION SIZE NEEDED IS ABOUT 150K + 4*(SIZE OF BLANK
COMMON IN WORDS)

C * * NOTE - THE ORDER OF COMMONS IN THIS ROUTINE IS IMPOR-
TANT AND MUST

C CORRESPOND TO THE ORDER USED IN DUMP ROUTINES SUCH AS
HELP,

C XSCHLP, AND USRHLP

C * *

C * * LABELLED COMMONS FOR WALK ROUTINES * * * * *

* * * * *

COMMON /APOLLO/ AGSTRT,DDF,DEADWT(26),ITOUT,ITIN

COMMON /FISBNK/ MFISTF

COMMON /NUTRON/ NAME

C * * LABELLED COMMONS FOR CROSS SECTION ROUTINES * * * * *

* * * * *

COMMON /LOCSIG/ISCCOG

```

COMMON /MEANS/ NM
COMMON /MOMENT/ NMOM
COMMON /QAL/ Q
COMMON /RESULT/ POINT

C * * LABELLED COMMONS FOR GEOMETRY INTERFACE ROUTINES * *
* * * * *
COMMON /GEOMC/ XTWO
COMMON /NORMAL/ UNORM

C * * LABELLED COMMONS FOR USER ROUTINES * * * * *
* * * * *
COMMON /PDET/ ND
COMMON /USER/ AGST

C * * COMMON /DUMMY/ WILL NOT BE FOUND ELSEWHERE IN THE
PROGRAM * * *
COMMON /DUMMY/ DUM
CHARACTER*20, NAM1
CHARACTER*20, NAM2
TYPE *, 'YOU ARE USING MORSEB AS MODIFIED BY M HERTE'
TYPE *, 'THIS VERSION USES A POINT SOURCE AT THE
ORIGIN'
TYPE *, 'AND ALBEDO BOUNDARY TO SIMULATE A PLANAR
SOURCE'
TYPE *, 'ENTER NAME OF INPUT FILE:'

```

```

        ACCEPT 100, NAM1
100    FORMAT(A20)
        TYPE 101, NAM1
101    FORMAT(X,A20)
        TYPE *, 'ENTER NAME OF OUTPUT FILE:'
        ACCEPT 200, NAM2
        TYPE 101, NAM2
200    FORMAT (A20)
        OPEN(UNIT=1,NAME=NAM1,TYPE='OLD')
        OPEN(UNIT=2,NAME=NAM2,TYPE='NEW')
        ITOUT = 2
        ITIN = 1
        NLFT=199999
        CALL MORSE(NLFT)
        TYPE 300, NAM2
300    FORMAT(X, 'OUTPUT FILE IS ',A20)
        STOP
        END

```

C.2 BDRYX

BDRYX is a subroutine called when particles encounter a change in media. It also performs fluence estimation if the source to collision distance corresponds to a detector position.

SUBROUTINE BDRYX

C IDENTIFIES DETECTOR POSITION WITH A BOUNDARY CROSSING
AND THEN

C CALCULATES AND SUMS QUANTITIES OF INTEREST FOR EACH
BATCH.

C

COMMON /USER/ AGSTRT,WTSTRT,XSTRT,YSTRT,ZSTRT,DFP,E-
BOTN,EBOTG,

1 TCUT,IO,I1,IADJM,NGPQT1,NGPQT2,NGPQT3,NGPQTG,NGPQTN,N
ITS,NLAST,

2 NLEFT,NMGP,NMTG,NSTRT

COMMON /PDET/
ND,NNE,NE,NT,NA,NRESP,NEX,NEXND,NEND,NDNR,NTNR,NTNE,

1 NANE,NTNDNR,NTNEND,NANEND,LOCRSP,LOCXD,LOCIB,LOCCO,LO
CT,LOCUD,

2 LOCSD,LOCQE,LOCQT,LOCQTE,LOCQAE,LMAX,EFIRST,EGTOP

COMMON /NUTRON/ NAME,NAMEX,IG,IGO,NMED,ME-
DOLD,NREG,U,V,W,UOLD,VOLDBEDRY

1 ,WOLD,X,Y,Z,XOLD,YOLD,ZOLD,WATE,OLDWT,WTBC,BLZNT,BLZO
N,AGE,OLDAGEBDRY

DATA ABDX/1.0E10/,ZBDX/100./

Z1 = ZBDX+.1

Z2 = ZBDX-.1

IF ((Z.GT.Z2).AND.(Z.LT.Z1)) THEN

ABCOS=ABS (W)

IF (ABCOS.LT.0.01) ABCOS=0.005

CON=WATE/ABCOS/ABDX

CALL FLUXST(1,IG,CON,AGE,0,0)

ENDIF

RETURN

END

C.3 BANKR

BANKR is a subroutine used to call the appropriate user specified diagnostic subroutine.

SUBROUTINE BANKR(NBNKID)

C DO NOT CALL EUCLID FROM BANKR(7)

COMMON /APOLLO/ AGSTRT,DDF,DEADWT(5),ETA,ETATH,E-
TAUSD,UINP,VINP,

1 WINP,WTSTRT,XSTRT,YSTRT,ZSTRT,TCUT,XTRA(10),

2 IO,I1,MEDIA,IADJM,ISBIAS,ISOUR,ITERS,ITIME,ITSTR,LO
CWTS,LOCFWL,

3 LOCEPR,LOCNSC,LOCFSN,MAXGP,MAXTIM,ME-
DALB,MGPREG,MXREG,NALB,

4 NDEAD(5),NEWNM,NGEOM,NGPQT1,NGPQT2,NGPQT3,NGPQTG,NGPQ
TN,NITS,

5 NKCALC,NKILL,NLAST,NMEM,NMGP,NMOST,NMTG,NO-
LEAK,NORMF,NPAST,

6 NPSCL(13),NQUIT,NSIGL,NSOUR,NSPLT,NSTRT,NXTRA(10)

COMMON /NUTRON/ NAME,NAMEX,IG,IGO,NMED,ME-
DOLD,NREG,U,V,W,UOLD,VOLD

1 ,WOLD,X,Y,Z,XOLD,YOLD,ZOLD,WATE,OLDWT,WTBC,BLZNT,BLZO
N,AGE,OLDAGE

NBNK = NBNKID

IF (NBNK) 100,100,140

```

100 NBNK = NBNK + 5
      GO TO (104,103,102,101),NBNK
101 CALL STRUN
C     CALL HELP(4HSTRU,1,1,1,1)
      RETURN
102 NBAT = NITS - ITERS
      NSAVE = NMEM
      CALL STBTCH(NBAT)
C     NBAT IS THE BATCH NO. LESS ONE
      RETURN
103 CALL NBATCH(NSAVE)
C     NSAVE IS THE NO. OF PARTICLES STARTED IN THE LAST
BATCH
      RETURN
104 CALL NRUN(NITS,NQUIT)
C     NITS IS THE NO. OF BATCHES COMPLETED IN THE RUN JUST
COMPLETED
C     NQUIT .GT. 1 IF MORE RUNS REMAIN
C           .EQ. 1 IF THE LAST SCHEDULED RUN HAS BEEN
COMPLETED
C           IS THE NEGATIVE OF THE NO. OF COMPLETE RUNS,
WHEN AN
C           EXECUTION TIME KILL OCCURS

```

RETURN

140 GO TO (1,2,3,4,5,6,7,8,9,10,11,12,13),NBNK

C	NBNKID	COLL TYPE	BANKR CALL	NBNKID	COLL TYPE
			BANKR CALL		
C	1	SOURCE	YES (MSOUR)	2	SPLIT
			NO (TESTW)		
C	3	FISSION	YES (FPROB)	4	GAMGEN
			YES (GSTORE)		
C	5	REAL COLL	YES (MORSE)	6	ALBEDO
			YES (MORSE)		
C	7	BDRYX	YES (NXTCOL)	8	ESCAPE
			YES (NXTCOL)		
C	9	E-CUT	NO (MORSE)	10	TIME KILL
			NO (MORSE)		
C	11	R R KILL	NO (TESTW)	12	R R SURV
			NO (TESTW)		
C	13	GAMLOST	NO (GSTORE)		

1 RETURN

2 RETURN

3 RETURN

4 RETURN

5 RETURN

6 RETURN

7 CALL BDRYX
RETURN
8 RETURN
9 RETURN
10 RETURN
11 RETURN
12 RETURN
13 RETURN
END

C.4 SOURCE

This is a version of the SOURCE subroutine used by MORSE to assign initial parameters to all primary particles.

```
      SUBROUTINE SOURCE(IG,U,V,W,X,Y,Z,WATE,MED,AG,I-  
SOUR,ITSTR,NGPQT3,
```

```
1   DDF,ISBIAS,NMTG)
```

```
      COMMON /USER/ DUM(9),IO,I1,IDUM(12)
```

```
      COMMON WTS(1)
```

C

C IF ITSTR=0, MUST PROVIDE IG,X,Y,Z,U,V,W,WATE AND AG IF
DESIRED TO BE

C DIFFERENT FROM CARD VALUES (WHICH ARE THE VALUES INPUT
TO SOURCE)

C IF ITSTR=1, IG IS THE GRP NO. CAUSING FISSION, MUST
PROVIDE NEW IG

C THIS VERSION OF SOURCE SELECTS INITIAL GROUP FROM
THE INPUT SPEC

C

```
      DATA ICALL/1/
```

```
      IF (ICALL) 10,10,5
```

```
5   ICALL = 0
```

```
      WRITE (IO,1000)
```

```
1000 FORMAT (' YOU ARE USING THE DEFAULT VERSION OF SOURCE
```

WHICH SETS W

1ATE TO DDF AND PROVIDES AN ENERGY IG.')

10 IF(ISOOR)15,15,60

15 WATE=DDF

IF (ISBIAS) 20,20,25

20 NWT = 2*NMTG

GO TO 30

25 NWT = 3*NMTG

30 R = FLTRNF(0)

DO 35 I=1,NGPQT3

IF (R - WTS(I+NWT)) 40,40,35

35 CONTINUE

40 IG=I

IF (ISBIAS) 60,60,45

45 IF (I-1) 60,50,55

50 WATE = WATE*WTS(2*NMTG+1)/WTS(3*NMTG+1)

GO TO 60

55 WATE = WATE*(WTS(2*NMTG+I)-WTS(2*NMTG+I-

1)))/(WTS(3*NMTG+I)-WTS(3*N

1MTG+I-1))

C *****

C This version of the MORSE SOURCE file is for a POINT

source

c AT THE ORIGIN OF THE X, Y PLANE WITH VARIABLE Z, AS
GIVEN IN INPUT

C *****

60 Y = 0.0

 X = 0.0

100 RETURN

 END

C.5 XCHKR Input

XCHKR is a routine for mixing macroscopic cross sections. The routine uses information from the file reproduced below, in conjunction with the appropriate microscopic cross section data contained in the FEWG1 library, to produce the macroscopic cross sections for each zone in the MORSE problem. The input file shown here was used to mix the cross sections for the shielding material contained in the asphalt shingles (calcium carbonate) and the surrounding soil and air.

```
0    3    21    21
21 gamma (P3) for Thesis//Soil, AIR and CaCO3 Dec 90
    0    0    21    21    58    61    4    3    8    10    4    2
1    3
    0    0    0    0    0    0    0    10    15    0    0
    2    3    4    5    30    31    32    33    38    39    40    41
42    43
    44    45    62    63    64    65    66    67    68    69    78    79
80    81
150  151  152  153
    1    3  4.199E-5      N(38) \
    1    4  1.128E-5      O(42)  > AIR @ STP
    1   -8  2.515E-7      AR(150)/
```

2	1	9.752E-3	H(2) \
2	4	3.480E-2	O(42) \
2	5	4.880E-3	AL(62) / SOIL
2	-6	1.160E-2	SI(66)/
3	7	3.333E-3	Ca(78)\
3	2	3.333E-3	C (30) >Asphalt Aggregate
(CaCO3)			
3	-4	1.000E-2	O (42)/

APPENDIX C: Sample MORSE Input

This is a sample of a typical input parameters file read by the MORSE transport code.

DISTRIBUTED SOURCE, AIR & GROUND, DOSE AT 1m ABOVE
GROUND, MORSE

```
1000 4001 100 1 0 21 21 21 0 0 450. 3
4
-1 21 0 0 1.0 0 1.0E+4 0.0
0
0.0 0.0 -2.11E-2 0.0 0.0 0.0
0.0
0.0000-00 0.0000-00 8.8363-15 1.7673-14 1.1231-08 9.1822-05
5.2470-03
1.5715-02 4.2570-02 6.5522-02 1.3979-01 2.4577-01 1.5558-01
1.1395-01
1.2497-01 4.3594-02 2.0224-02 1.6857-02 1.0115-02 0.0000-00
0.0000-00
1.4000 +7 1.0000 +7 8.0000 +6 7.0000 +6 6.0000 +6 5.0000 +6
4.0000 +6
3.0000 +6 2.5000 +6 2.0000 +6 1.5000 +6 1.0000 +6 7.0000 +5
4.5000 +5
3.0000 +5 1.5000 +5 1.0000 +5 7.0000 +4 4.5000 +4 3.0000 +4
2.0000 +4
```

8 A1C032E

	1	1	0	0	0	7	21		
	0	0	0	1	1	1		0.5	0.01 1.0
0.0									
	0	0	0	2	1	2		.75	0.05 1.0
0.0									
	0	0	0	3	1	3		1.0	0.05 1.0
0.0									
	0	0	0	4	1	4		1.0	0.10 1.0
0.0									
	0	0	0	5	1	5		1.0	0.10 1.0
0.0									
	0	0	0	6	1	6		1.0	0.10 1.0
0.0									

-1

0 0 0 0

0 0

TEST CASE FOR THESIS

RPP	-5.0E+4	5.0E+4	-5.0E+4	5.0E+4	-1.0E-9
1.0E+2					
RPP	-5.0E+4	5.0E+4	-5.0E+4	5.0E+4	-1.0E-9
0.1E+5					
RPP	-5.0E+4	5.0E+4	-5.0E+4	5.0E+4	-1.0E-9
0.5E+5					

RPP	-5.0E+4	5.0E+4	-5.0E+4	5.0E+4	-1.0E-9
1.0E+5					
RPP	-5.0E+4	5.0E+4	-5.0E+4	5.0E+4	-1.0E-9
4.0E+5					
RPP	-5.0e+4	5.0e+4	-5.0e+4	5.0e+4	-2.0E-2
4.0e+5					
RPP	-5.0e+4	5.0e+4	-5.0e+4	5.0e+4	-1.5e+3
4.0e+5					
RPP	-5.5e+4	5.5e+4	-5.5e+4	5.5e+4	-1.5e+3
4.0e+5					
RPP	-6.5e+7	6.5e+7	-6.5e+7	6.5e+7	-5.5e+7
5.5e+7					

END

1	+1	
2	+2	-1
3	+3	-2
4	+4	-3
5	+5	-4
6	+6	-5
7	+7	-6
8	+8	-7
9	+9	-8

END

1 1 2 3 4 5 6 7 7

1 1 1 1 1 2 3 4 0

21 GROUP GAMMA CROSS SECTIONS ---- AIR AND GROUND---ENC 3

0 0 21 21 58 61 4 3 8 10 4 1

1

1 0 0 0 0 0 0 -10 0 0 0

SAMBO ANALYSIS INPUT DATA FOR SCC (GAMMAS)

1 0 0 0 0 1 1 1

0.000 +0.0 1.0000E+2

(NORMALIZED PER SINGLE GAMMA FROM THE SOURCE)

PHOTON DOSE (RADS TISSUE/GAMMA/CM²)

3.2081E-9 2.4722E-9 2.0847E-9 1.8651E-9 1.6613E-9 1.4431E-9
1.1971E-9
1.0111E-9 8.707E-10 7.253E-10 5.641E-10 4.106E-10 2.930E-10
1.923E-10
1.106E-10 5.482E-11 3.711E-11 3.472E-11 6.327E-11 1.416E-10
4.406E-10

\$\$\$\$\$\$\$\$\$ MORSE6.FOR PROBLEM ***** Asphalt.in *****

APPENDIX D: Gamma Source Emission Rates

This table gives a twenty one group format of the gamma emission rates of the three fission product chains calculated by Millage. The restructuring from nineteen groups to twenty one groups was required to use the FEWG1 cross sections.

U-235	Pu-239	U-238
0.000E+00	0.000E+00	0.000E+00
0.000E+00	0.000E+00	0.000E+00
1.354E-18	1.501E-18	2.042E-08
2.708E-18	3.001E-18	4.085E-08
1.721E-12	1.094E-12	4.071E-07
1.407E-08	8.153E-09	1.879E-06
8.040E-07	1.012E-06	3.486E-06
2.408E-06	2.004E-06	1.032E-05
6.523E-06	5.143E-06	1.455E-05

U-235	Pu-239	U-238
1.004E-05	9.603E-06	1.194E-05
2.142E-05	1.957E-05	1.179E-05
3.766E-05	3.642E-05	6.820E-06
2.384E-05	2.422E-05	7.381E-06
1.746E-05	2.047E-05	1.555E-06
1.915E-05	2.192E-05	7.182E-06
6.680E-06	6.457E-06	1.741E-11
3.099E-06	3.264E-06	1.840E-16
2.583E-06	2.720E-06	1.534E-16
1.550E-06	1.632E-06	9.202E-17
0.000E+00	0.000E+00	0.000E+00
0.000E+00	0.000E+00	0.000E+00

APPENDIX E: Davies McDonald Fall Mechanics Code

This is the BASIC code used to calculate the particle fall-times shown in Figure 3.

```
100 REM * CALCULATION OF FALLOUT ARRIVAL TIMES USING
MCDONALD-DAVIES *
110 INPUT "SIZE IN MICRONS";R
130 INPUT "INITIAL ALTITUDE IN METERS";Z
135 PRINT "RADIUS = ";R;" MICRONS","INITIAL ALTITUDE = ";Z;"
METERS"
138 R = R*.000001
140 DZ0 = 100: G = 9.8: DF = 2600
145 PRINT "Z","Q","REY #", "VZ", "TIME(HRS)"
148 DZ = DZ0
150 GOSUB 800
160 Q = 32*D*DF*G*R^3/(3*VIS*VIS)
170 PRINT Z,Q,
175 QQ = LOG(Q)/LOG(10)
180 IF Q < 100 THEN REY = Q/24 -2.3363E-04*Q^2 +2.0154E-
06*Q^3-6.9105E-09*Q^4      ELSE REY = -1.29536+.986*QQ
-.046677*QQ^2+.0011235*QQ^3
190 IF Q => 100 THEN REY = 10^(REY)
200 VZ = REY*VIS/(2*D*R)
205 VZ = VZ*(1 + 1.165E-07/(R*D))
```

```

210 DT = DZ/VZ
220 TA = TA + DT
225 PRINT REY,VZ,TA/3600
228 IF Z = 0 THEN STOP
230 Z = Z - DZ
240 IF Z > 0 THEN 150
250 IF DZ <> DZO THEN STOP
260 DZ = DZ + Z : Z = 0
270 GOTO 150

800 REM * US STANDARD ATMOSPHERE *
810 REM * ENTER WITH ALTITUDE Z IN METERS *
820 P0 = 101300!
830 IF Z < 11000 THEN T = 288.15 - .006545*Z : P =
P0*(288.15/T)^(-.034164/.006545)
840 IF ( Z >= 11000) AND ( Z < 20000) THEN T = 216.65 : P =
22690!*EXP(-.034164*(Z-11000)/216.65)
850 IF ( Z >= 20000) AND ( Z < 32000) THEN T = 216.65 +
.001*(Z-20000) : P = 5528*(216.65/T)^(.034164/.001)
860 IF ( Z >= 32000) AND ( Z < 47000!) THEN T = 228.65 +
.0028*(Z-32000) : P = 888.8*(228.65/T)^(.034164/.0028)
870 IF ( Z >= 47000!) AND ( Z < 52000!) THEN T = 270.65 : P =
115.8*EXP(-.034164*(Z-47000!)/T)
880 IF ( Z >=52000!) AND ( Z< 61000!) THEN T = 270.65 -.002*(Z

```

```
- 52000!) : P = 62.21*(270.65/T)^(-.034164/.002)
890 IF (Z >= 61000!) THEN PRINT "Z OUT OF RANGE"
900 D = .003484*P/T
910 S = SQR(401.86*T)
920 VIS = 1.458E-06*T^1.5/(T+110.4)
930 MI = .10197*P
940 REM * OUPUT = T,P,D,S,VIS,MI *
950 RETURN
```

Bibliography

1. Baker, G. H. III, Implications of Atmospheric Test Fallout Data For Nuclear Winter, Unpublished Disertation, Air Force Institue of Technology, Wright-Patterson AFB, OH, 1987.
2. Bartine, D. And others, 37 Neutron, 21 Gamma Ray coupled, P3. Multigroup Library in ANLSN Format, DLC-31, Oak Ridge National Laboratory, Oak Ridge, TN, 1979.
3. Bridgman, Charles J., Class Notes from NENG 635, The Physics and Effects pf Nuclear Explosives, Residual Radiation, School of Engineering, Air Force Institute of Technology, Wright-Patterson AFB, Oh, 1989.
4. Bridgman, Charles J., Air Force Institue of Technology, Wright-Patterson AFB, OH, private communication, Nov 1990.
5. Cashwell, E. D. And Everett, C. J., A Practical Manual on the Monte Carlo Method for Random Walk Problems, LA-2120, Los Alamos National Laboratory, Los Alamos, NM, 1957.
6. Cramer, S. N., Applications Guide to the MORSE Monte Carlo Code, ORNL/TM-9355, Oak Ridge National Laboratory, Oak Ridge, TN, 1985.

7. Emmett, M. B., General Purpose Monte Carlo Multigroup Neutron and Gamma-Ray Transport Code with Combinational Geometry, CCC-203, Oak Ridge National Laboratory, Oak Ridge, TN, July 1984.
8. French, R. L. And others, Ground Roughness Effects on Fallout Shielding, NRDL TRC-68-5, 1968.
9. Glasstone, Samuel and Dolan, Philip J., The Effects of Nuclear Weapons, Washington DC, Government Printing Office, 1977.
10. Howard, Michael R., Monte Carlo Determination of Gamma Ray Exposure From a Homogeneous Ground Plane, Unpublished Thesis, Air Force Institute of Technology, Wright-Patterson AFB, OH, 1990.
11. Knoll, Glenn F., Radiation Detection and Measurement, John Wiley and Sons, New York, 1979.
12. Millage, Kyle K., Fission Product Decay Characteristics, Unpublished Thesis, Air Force Institute of Technology, Wright-Patterson AFB, OH, 1989.
13. Walker, William F. And others, Chart of the Nuclides (13th edition), General Electric company, San Jose, CA, 1984.
14. Weisman, Joel, Elements of Nuclear Reactor Design (Second Edition), Krieger Publishing, Malabar, FL, 1983.

15. Wittington, Mark, Georgia Pacific Corporation, Gypsum and Roofing Division, Atlanta, GA, Telephone Interview, Nov 1990.

16. Wood, James, Computational Methods in Reactor Shielding, Pergamon Press, New York, 1982.

Vita

Mark S. Herte was born on 11 November 1958 in Medina, Ohio. He graduated from North East High School, Lincoln, Nebraska in 1977. In August 1986, he received his Bachelor of Science degree in Nuclear Engineering through the Air-men's Education and Commissioning Program (AECPP) at the University of Florida. He was commissioned in December 1986 as a distinguished graduate of the U S Air Force Officer's Training School, and was assigned to the Air Force Weapons Lab, Kirtland Air Force Base, New Mexico. Captain Herte entered the Nuclear Engineering graduate program at the Air Force Institute of Technology in August 1989.

Permanent address: 13307 Old Mill Road
Spencer, OH 44275

REPORT DOCUMENTATION PAGE

Form Approved
OMB No. 0704-0188

Public reporting burden for this collection of information is estimated to average 1 hour per response, including the time for reviewing instructions, searching existing data sources, gathering and maintaining the data needed, and completing and reviewing the collection of information. Send comments regarding this burden estimate or any other aspect of this collection of information, including suggestions for reducing this burden, to Washington Headquarters Services, Directorate for Information Operations and Reports, 1215 Jefferson Davis Highway, Suite 1204, Arlington, VA 22202-4302, and to the Office of Management and Budget, Paperwork Reduction Project (0704-0188), Washington, DC 20503.

1. AGENCY USE ONLY (Leave blank)		2. REPORT DATE March 1991	3. REPORT TYPE AND DATES COVERED Master's Thesis	
4. TITLE AND SUBTITLE The Self-shielding of Fallout Gamma Rays by Terrain Roughness			5. FUNDING NUMBERS	
6. AUTHOR(S) Mark S. Herte, Capt, USAF				
7. PERFORMING ORGANIZATION NAME(S) AND ADDRESS(ES) Air Force Institute of Technology, WPAFB OH 45433-6583			8. PERFORMING ORGANIZATION REPORT NUMBER AFIT/GNE/ENP/91M-2	
9. SPONSORING / MONITORING AGENCY NAME(S) AND ADDRESS(ES)			10. SPONSORING / MONITORING AGENCY REPORT NUMBER	
11. SUPPLEMENTARY NOTES				
12a. DISTRIBUTION / AVAILABILITY STATEMENT Approved for public release; distribution unlimited			12b. DISTRIBUTION CODE	
13. ABSTRACT (Maximum 200 words) The study presents a first order calculation of the self-shielding of nuclear weapon fission fragment gamma rays by surface roughness (microscopic terrain irregularities). To simulate fallout particles, polymer microspheres were deposited on slides containing samples of soil, concrete and asphalt roofing shingles. Scanning electron microscopy was used to photographically map the surfaces. The thickness of surface irregularities at various angles was measured by converting the photographs to digital images. Measurements showed a dependence upon the surface type, but not upon particle size. Average values of the measurements were modelled using a homogeneous buried source. With this geometry, dose rates were calculated using the Monte Carlo transport code, MORSE. The MORSE calculations showed self-shielding due to roughness of not more than five percent for the soil samples and eight percent for the shingles. The 30 percent self-shielding used in <u>The Effects of Nuclear Weapons</u> for level terrain is six times as great. It is postulated the large attenuation formerly attributed to roughness may actually be an artifact of an incorrect global/local fallout partition.				
14. SUBJECT TERMS Fallout, Terrain Roughness, and Radiation Shielding			15. NUMBER OF PAGES 101	
			16. PRICE CODE	
17. SECURITY CLASSIFICATION OF REPORT Unclassified	18. SECURITY CLASSIFICATION OF THIS PAGE Unclassified	19. SECURITY CLASSIFICATION OF ABSTRACT Unclassified	20. LIMITATION OF ABSTRACT UL	